



Cholic Acid-Peptide Conjugates as Potent Antimicrobials against Interkingdom Polymicrobial Biofilms

Siddhi Gupta,^a Jyoti Thakur,^b Sanjay Pal,^{a,c} Ragini Gupta,^a Deepakkumar Mishra,^a Sandeep Kumar,^{a,d} Kavita Yadav,^{a,d} Amandeep Saini,^e Prabhu S. Yavvari,^b Madhukar Vedantham,^a Archana Singh,^f Aasheesh Srivastava,^b Rajendra Prasad,^e Avinash Bajaj^a

^aLaboratory of Nanotechnology and Chemical Biology, Regional Centre for Biotechnology, NCR Biotech Science Cluster, Faridabad, Haryana, India

^bDepartment of Chemistry, Indian Institute of Science Education and Research, Bhopal, Madhya Pradesh, India

^cKalinga Institute of Industrial Technology, Bhubaneswar, Odisha, India

^dManipal Academy of Higher Education, Manipal, Karnataka, India

^eAmity Institute of Integrative Sciences and Health, Amity University, Gurugram, Haryana, India

^fCSIR-Institute of Genomics and Integrative Biology, New Delhi, India

ABSTRACT Interkingdom polymicrobial biofilms formed by Gram-positive *Staphylococcus aureus* and *Candida albicans* pose serious threats of chronic systemic infections due to the absence of any common therapeutic target for their elimination. Herein, we present the structure-activity relationship (SAR) of membrane-targeting cholic acid-peptide conjugates (CAPs) against Gram-positive bacterial and fungal strains. Structure-activity investigations validated by mechanistic studies revealed that valine-glycine dipeptide-derived CAP 3 was the most effective broad-spectrum antimicrobial against *S. aureus* and *C. albicans*. CAP 3 was able to degrade the pre-formed single-species and polymicrobial biofilms formed by *S. aureus* and *C. albicans*, and CAP 3-coated materials prevented the formation of biofilms. Murine wound and catheter infection models further confirmed the equally potent bactericidal and fungicidal effect of CAP 3 against bacterial, fungal, and polymicrobial infections. Taken together, these results demonstrate that CAPs, as potential broad-spectrum antimicrobials, can effectively clear the frequently encountered polymicrobial infections and can be fine-tuned further for future applications.

KEYWORDS antibacterial, antifungal, antimicrobials, bile acids, biofilms, membrane targeting

Biofilms formed on medical implants or infected tissues are usually complex, diverse, heterogeneous, and polymicrobial in nature, where microbes from different species and genera evolve a mutualistic or synergistic relationship through physical and chemical interactions (1). These interactions help the microorganisms cohabit on epithelial surfaces and on indwelling medical devices (1). Sessile communities of microorganisms grown on a substratum or tissue can act as major mediators of systemic infections. These biofilms help in the enrichment of nutrients in their extracellular matrix and also enable them to evade the antibiotic treatment and host defense mechanism (2–4). Migration of detached microcolonies from biofilms to uninfected tissues can allow the formation of biofilms at distant sites and can cause persistent chronic recurrent systemic infections (5).

Candida albicans, the most prevalent of all fungal pathogens, is the fourth leading cause of bloodstream infections that readily forms biofilms on indwelling medical devices such as dental materials, stents, prostheses, implants, endotracheal tubes, pacemakers, and catheters (6). *C. albicans* is also a part of ~25% of wound infections and contributes to 50% of the overall microbial burden (7). The majority of nosocomial

Citation Gupta S, Thakur J, Pal S, Gupta R, Mishra D, Kumar S, Yadav K, Saini A, Yavvari PS, Vedantham M, Singh A, Srivastava A, Prasad R, Bajaj A. 2019. Cholic acid-peptide conjugates as potent antimicrobials against interkingdom polymicrobial biofilms. *Antimicrob Agents Chemother* 63:e00520-19. <https://doi.org/10.1128/AAC.00520-19>.

Copyright © 2019 American Society for Microbiology. All Rights Reserved.

Address correspondence to Siddhi Gupta, siddhi.gupta@rcb.res.in, or Avinash Bajaj, bajaj@rcb.res.in.

S.G. and J.T. contributed equally to this work.

Received 11 March 2019

Returned for modification 2 June 2019

Accepted 10 August 2019

Accepted manuscript posted online 19 August 2019

Published 22 October 2019

C. albicans infections are polymicrobial in nature, where *Staphylococcus aureus*, a Gram-positive bacteria, is one of the most commonly available bacterial pathogens (3, 8). These interkingdom relations in *S. aureus*-*C. albicans* polymicrobial biofilms can be maintained by contact-dependent attachment and cell-cell communication (8). Polymicrobial interactions in biofilms help the microorganisms develop resistance against host defense mechanisms and antimicrobial therapies (9, 10). Therefore, there is an urgent need to study the mechanisms of drug resistance developed by these polymicrobial biofilms and to develop antimicrobials against these polymicrobial biofilms (11).

Current therapies for the treatment and prevention of these polymicrobial biofilm-mediated infections include surgical interventions, prolonged antibiotic treatment, or the addition of antimicrobial agents to medical devices (12). Chemotherapeutic treatment of these polymicrobial biofilms needs a combination of antibiotics, as the cells (*S. aureus* and *C. albicans*) constituting these biofilms present distinct cellular targets and phenotypic as well as genetic expressions (13, 14). Recent studies have shown that combinations of antibacterial and antifungal antimicrobials show very poor efficacy against *C. albicans*-*S. aureus* cobiofilms, and this approach of combination therapy usually fails in ~70% of infections (15).

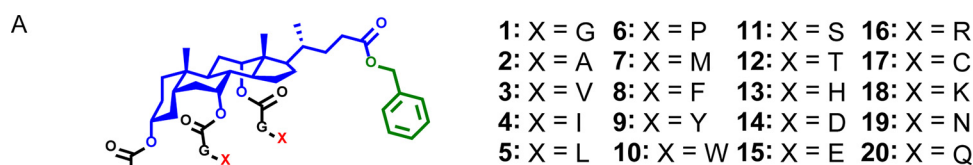
Antimicrobial and antimycotic peptides (AMPs) are a first line of defense that are present in prokaryotes and eukaryotes (16, 17). These AMPs usually form α -helix- or β -sheet-enriched structures giving them an amphipathic character. The membrane-binding nature and ability to lyse the microbes allow these peptides to have broad-spectrum antimicrobial activity, where positive residues perform electrostatic interactions with membranes followed by intercalation and membrane rupturing (18). Lipopeptides such as echinocandins or histidine-rich peptides disrupt the fungal membranes (19), and peptides such as magainins and protegrins are antibacterial in nature (20). Inspired by the design of these AMPs, numerous small molecules (21), lipopeptides (22), and cationic steroidal amphiphiles (23) targeting the bacterial and fungal membranes have been synthesized and screened for their activity, but none of these studies have ever reported the activity of amphiphiles on polymicrobial biofilms (24, 25).

Cholic acid (CA) is a naturally occurring facial amphiphile mimicking the amphiphilic nature of AMPs (26). Numerous CA-derived amphiphiles have been engineered for antimicrobial activity, and it has been shown that these amphiphiles, similar to AMPs, interact with bacterial membranes and cause membrane disruptions (27–29). Recently, we have shown that conjugation of dipeptide units on a CA backbone helps in effective interactions with lipopolysaccharide and in combating Gram-negative bacterial infections (30). In this article, we present the screening of these conjugates against Gram-positive bacterial and fungal strains and show that valine-glycine-derived CAP 3 has a broad-spectrum antimicrobial activity and is also able to disrupt *S. aureus*, *C. albicans*, and polymicrobial biofilms in murine models.

RESULTS AND DISCUSSION

Antimicrobial activity against Gram-positive bacterial and fungal strains.

Twenty cholic acid-peptide conjugates (CAPs) with general chemical formula of CA-(G-X)₃ were used, where G is glycine and X is any natural amino acid (Fig. 1A) (30). We tested the antibacterial efficacy of the CAPs against different Gram-positive bacterial strains (*S. aureus*, *Bacillus subtilis* and *Streptococcus pneumoniae*) using a broth dilution assay and determined the MIC_{99.5} (Fig. 1B) (31). Valine (V)- and isoleucine (I)-derived amphiphiles CAP 3 and CAP 4 were most active against all three Gram-positive bacteria at 8 μ M. All MIC₉₉, MIC₈₀, and cytotoxicity values in micrograms per milliliter are mentioned in Table S1 posted at <https://rcb.res.in/upload/Revised%20SI%20PR%20MS.pdf>. Activities of CAPs were then tested against different fungal strains of *Candida* (*C. albicans*, *C. tropicalis*, and *C. kefyr*) to determine the MIC₈₀ (32). In general, CAPs were found to be more active against fungal strains than bacterial strains, and those based on hydrophobic amino acids such as glycine (CAP 1), alanine (CAP 2), valine (CAP 3), isoleucine (CAP 4), leucine (CAP 5), and proline (CAP 6) were active in the range of 2 to 8 μ M (Fig. 1B). CAPs 3 and 4 have an MIC₈₀ of 4 μ M against *C. albicans* and showed



G = Glycine, X = any natural amino acid

B

| | | MIC ₉₉ (μM) ^a (Gram-positive bacteria) | | | MIC ₈₀ (μM) ^b (<i>Candida</i> strains) | | | IC ₅₀ (μM) ^c |
|-------------|-------------------|---|--------------------|----------------------|--|----------------------|-----------------|------------------------------------|
| CAPs | | <i>S. aureus</i> | <i>B. subtilis</i> | <i>S. pneumoniae</i> | <i>C. albicans</i> | <i>C. tropicalis</i> | <i>C. kefyr</i> | A549 |
| CAP 1 | CA-G ₃ | 128 | 64 | 32 | 4 | 8 | 4 | >100 |
| CAP 2 | CA-A ₃ | 128 | 64 | 16 | 4 | 4 | 2 | 76.39 |
| CAP 3 | CA-V ₃ | 8 | 8 | 8 | 4 | 4 | 2 | 56.42 |
| CAP 4 | CA-I ₃ | 8 | 8 | 8 | 4 | 8 | 2 | 7.68 |
| CAP 5 | CA-L ₃ | 32 | 32 | 8 | 8 | 4 | 4 | 9.88 |
| CAP 6 | CA-P ₃ | 128 | 128 | 16 | 8 | 8 | 2 | >100 |
| CAP 7 | CA-M ₃ | 16 | 16 | 64 | 4 | 8 | 4 | 58.66 |
| CAP 8 | CA-F ₃ | >256 | >256 | 64 | 8 | 8 | 4 | 4.35 |
| CAP 9 | CA-Y ₃ | >256 | >256 | >256 | 16 | >256 | 4 | >100 |
| CAP 10 | CA-W ₃ | >256 | >256 | >256 | >256 | >256 | 128 | >100 |
| CAP 11 | CA-S ₃ | 128 | 128 | 64 | 8 | 8 | 4 | >100 |
| CAP 12 | CA-T ₃ | 256 | 256 | 64 | 16 | 8 | 8 | >100 |
| CAP 13 | CA-H ₃ | 64 | 64 | 32 | 8 | 32 | 4 | >100 |
| CAP 14 | CA-D ₃ | >256 | >256 | >256 | >256 | >256 | >256 | >100 |
| CAP 15 | CA-E ₃ | >256 | >256 | >256 | >256 | >256 | >256 | >100 |
| CAP 16 | CA-R ₃ | 32 | >256 | 8 | 16 | >256 | 8 | >200 |
| CAP 17 | CA-C ₃ | >256 | >256 | 128 | >256 | >256 | 4 | >200 |
| CAP 18 | CA-K ₃ | >256 | 128 | 32 | 4 | 16 | 4 | >100 |
| CAP 19 | CA-N ₃ | >256 | >256 | >256 | 16 | 16 | 8 | >100 |
| CAP 20 | CA-Q ₃ | 128 | 128 | >256 | 32 | 32 | 32 | >100 |
| Polymyxin B | | 4 | 4 | 8 | — ^d | — ^d | — ^d | — ^d |
| Fluconazole | | — ^d | — ^d | — ^d | 4 | >256 | 26 | — ^d |

a: Minimum inhibitory concentration at which 99% bacterial growth inhibition was observed. b: Minimum inhibitory concentration at which 80% fungal growth inhibition was observed. c: Cytotoxic activity of CAPs against human lung epithelial (A549) cells as IC₅₀ the concentrations at which 50% cell death was observed. d: not determined.

FIG 1 (A) General molecular structure of cholic acid-peptide conjugates (CAPs) (1 to 20), where three hydroxyl groups were derivatized with dipeptides of -X-G- motif (X, any other natural amino acid; G, glycine) and the carboxyl terminus is modified with a benzyl group. (B) Table showing antibacterial and antifungal activities of CAPs (1 to 20) against different bacterial and fungal strains along with cytotoxicity activities of the amphiphiles against human lung epithelial cells. Cytotoxicity values were taken from reference 30.

broad-spectrum activity against Gram-positive bacterial and fungal strains. We tested the cytotoxicity of all the amphiphiles against human lung epithelial cells (A549) and found that CAP 4 is highly toxic to mammalian epithelial cells with a 50% inhibitory concentration (IC₅₀) of ~8 μM (30). In contrast, CAP 3 is less toxic to mammalian cells and showed >7-fold selectivity for Gram-positive bacteria and >15-fold selectivity for *C. albicans* over mammalian epithelial cells (Fig. 1B) (30). Therefore, we selected CAP 3 for further studies.

Membrane-targeted mechanism of action. To decipher the bactericidal effect of CAP 3 against *S. aureus*, bacteria were treated with 16 and 32 μM (2× and 4× MIC₉₉) CAP 3 and, at stipulated time intervals, bacteria were quantified by CFU assay. There was a 2-log reduction in the number of viable colonies within 30 min of treatment with CAP 3 at 32 μM, and 3 h of treatment with 32 μM CAP 3 was sufficient to clear the growth (Fig. 2A). To confirm the membrane-disrupting antibacterial mechanism of CAP 3, cytoplasmic membrane depolarization activity of CAP 3 against *S. aureus* was determined using membrane potential-sensitive 3,3'-diethylthiadicarbocyanine iodide dye [DiSC₂(5)] (33). DiSC₂(5) can cross the bacterial outer membranes and can accumulate in the cytoplasmic membranes. Disruption of the membrane potential allows

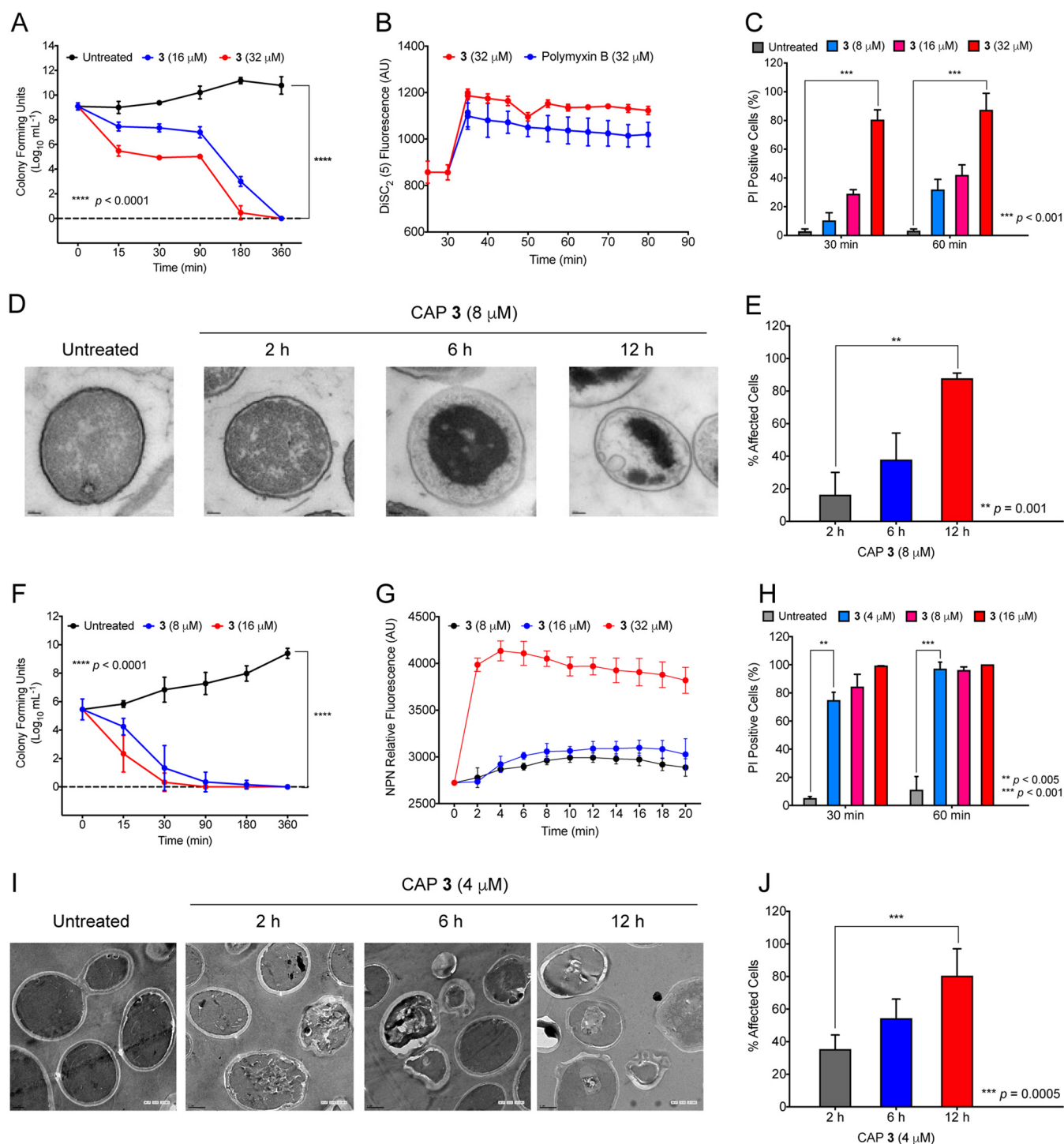


FIG 2 (A) Time-dependent killing on treatment of *S. aureus* with CAP 3 (16 and 32 μ M) reveals the bactericidal effect of CAP 3. Data are presented as means \pm SEMs from three biological replicates, and statistical analysis was performed using two-way analysis of variance (ANOVA). (B) Changes in fluorescence of DiSC₂(5) after treatment of *S. aureus* with CAP 3 (32 μ M) and polymyxin B (32 μ M) reveals the ability of CAP 3 to depolarize the bacterial membranes. Data are presented as means \pm SEMs from three biological replicates. (C) Percentages of propidium iodide (PI)-positive cells analyzed by flow cytometry after treatment of *S. aureus* with different doses (8, 16, and 32 μ M) of CAP 3 confirm its membrane-disrupting character. Data are presented as means \pm SEMs from three biological replicates, and statistical analysis was performed by unpaired two-tailed Student's *t* test. (D) Transmission electron micrographs of *S. aureus* at different time points (2, 6, and 12 h) after treatment with CAP 3 (8 μ M) show condensation of genomic material and disintegration of cell membrane compared to that in untreated bacteria. (E) Time-dependent quantification of the affected cells by transmission electron microscopy after treatment of *S. aureus* for different time points (2, 6, and 12 h) with CAP 3 (8 μ M). Data are presented as means \pm SDs from at least eight different images, and statistical analysis was performed by unpaired two-tailed Student's *t* test. (F) Time-dependent killing after treatment of *C. albicans* with CAP 3 (8 and 16 μ M) confirms fungicidal effect by CAP 3. Data are presented as means \pm SEMs from three biological replicates, and statistical analysis was performed using two-way ANOVA. (G) Changes in fluorescence of *N*-phenyl-1-naphthylamine (NPN) in labeled *C. albicans* cells after treatment with different concentrations of CAP 3 (8, 16, and 32 μ M) confirm (Continued on next page)

the release of the dye and enhances its fluorescence. There was an ~ 1.5 -fold increase in DiSC₂(5) fluorescence upon treatment of *S. aureus* with CAP 3 at 32 μM ($4\times \text{MIC}_{99}$) similar to that with polymyxin, thereby confirming the ability of CAP 3 to disrupt the potential of the bacterial membranes (Fig. 2B). The ability of CAP 3 to permeabilize the *S. aureus* membranes was further validated using a propidium iodide (PI) uptake assay, where CAP 3-treated cells (8, 16, and 32 μM) were stained with PI and analyzed by flow cytometry. There was a dose- and time-dependent increase in the number of PI-positive cells, as we observed $\sim 20\%$ PI-positive cells after a 30-min treatment with CAP 3 at 16 μM ($2\times \text{MIC}_{99}$) and $>80\%$ PI-positive cells after 60 min of treatment with 32 μM ($4\times \text{MIC}_{99}$) of CAP 3 (Fig. 2C). The untreated and CAP 3-treated bacteria (8 μM for 6 h) were labeled with SYTO 9-PI dye combination, where SYTO 9 stains bacteria with intact or compromised cell membranes, and impermeable PI can accumulate only in cells that are considered to be dead or dying (34). Microscopy studies confirmed that bacteria were able to take up PI within 1 h of treatment, confirming the membrane lytic nature of the amphiphile at 8 μM (see Fig. S1A posted at <https://rcb.res.in/upload/Revised%20SI%20PR%20MS.pdf>).

Time-dependent transmission electron microscopy (TEM) studies were performed to see the effect of CAP 3 on the architecture of *S. aureus* (Fig. 2D). CAP 3 at 8 μM ($1\times \text{MIC}_{99}$) induced perturbations in membranes of Gram-positive bacteria similarly to active AMPs (35). The untreated bacteria showed a smooth spherical morphology with intact membranes. After 2 h of treatment with CAP 3 at 8 μM ($1\times \text{MIC}_{99}$), the cytoplasmic content shrank toward the center, and the effect was more pronounced after 6 and 12 h of treatment (Fig. 2D). There was thinning of the bacterial membranes followed by rupturing that led to the release of the cytoplasmic content (Fig. 2D). Shrinking of cytoplasmic content might be due to an imbalance in osmotic pressure created in the cells upon treatment. Quantification of the affected cells by TEM studies confirmed that $>80\%$ of the cells showed membrane disruptions after 12 h of CAP 3 treatment at 8 μM ($1\times \text{MIC}_{99}$) (Fig. 2E).

The time- and dose-dependent killing effect of CAP 3 against *C. albicans* revealed that CAP 3 was able to clear the *C. albicans* within 90 min of treatment at 8 and 16 μM ($2\times$ and $4\times \text{MIC}_{80}$) (Fig. 2F). *N*-Phenyl-1-naphthylamine (NPN), a hydrophobic dye, is known to permeabilize disrupted fungal membranes, causing an increase in its fluorescence (36). Therefore, we assessed the ability of CAP 3 to disrupt the membrane structures of *C. albicans* using an NPN probe, where fungal cells were incubated with NPN and treated with different doses (8, 16, and 32 μM) of CAP 3. The dose-dependent increase in the fluorescence confirmed the membrane-disrupting effect of CAP 3 on fungal membranes (Fig. 2G). Similarly, we probed the ability of CAP 3-treated (4, 8, and 16 μM) *C. albicans* to take up the impermeable PI, and observed a time- as well as dose-dependent increase in the number of PI-positive cells (Fig. 2H). We observed $>70\%$ PI-positive cells after 30 min of treatment at 4 μM ($1\times \text{MIC}_{80}$), and 8 μM ($2\times \text{MIC}_{80}$) treatment for 60 min induced $>90\%$ PI-positive cells. Confocal micrographs of SYTO 9-PI stained *C. albicans* cells further confirmed its membrane-disrupting character, as a clear PI uptake by the cells was seen after 6 h of CAP 3 treatment at 4 μM (see Fig. S1B at the URL mentioned above).

Transmission electron micrographs of untreated *C. albicans* showed a typical healthy state with a regular and intact cell membrane. CAP 3 treatment for 2 h at 4 μM ($1\times \text{MIC}_{80}$) was sufficient to induce membrane disruptions and a notable change in the cellular shape (Fig. 2I) (37). A clearly ruptured cytoplasm along with pores in the outer

FIG 2 Legend (Continued)

membrane permeabilization of fungi by CAP 3. Data are presented as means \pm SEMs from three biological replicates. (H) Percentages of PI-positive *C. albicans* cells after treatment with different doses (4, 8, and 16 μM) of CAP 3 for 30 and 60 min confirm the membrane-disrupting character of CAP 3 for fungi. Data are presented as means \pm SEMs from three biological replicates, and statistical analysis was performed by unpaired two-tailed Student's *t* test. (I) Transmission electron micrographs of *C. albicans* at different time points (2, 6, and 12 h) after treatment with CAP 3 (4 μM) show disintegration of cell membrane compared to that of untreated cells. (J) Time-dependent quantification of affected *C. albicans* cells by transmission electron microscopy after treatment with CAP 3 (4 μM) for different times (2, 6, and 12 h). Data are presented as means \pm SDs from at least eight different images, and statistical analysis was performed by unpaired two-tailed Student's *t* test.

cell wall was observed after 6 h of treatment, with an increase in number of pores. Longer (12-h) exposure of *C. albicans* with CAP 3 allowed the burst of cytoplasmic content as indicated by the bulges formed in the membranes (Fig. 2I) (37). We observed >70% affected *C. albicans* after 12 h of treatment with 4 μ M CAP 3 (Fig. 2J).

Activity against drug-resistant strains. As microorganisms are known to develop antimicrobial drug resistance through the accumulation of mutations in antimicrobial target genes, the abilities of *S. aureus* and *C. albicans* to develop resistance against CAP 3 were tested. Bacterial/fungal strains were treated with CAP 3, and treated cultures were tested for MIC₉₉/MIC₈₀ of CAP 3 over multiple generations (38). *S. aureus* did not develop any resistance against CAP 3, as there was no change in MIC₉₉ (8 μ M) of CAP 3 over multiple generations whereas there was a multifold increase in MIC₉₉ of neomycin (see Fig. S2A at the above-mentioned URL). Antimicrobial activity of CAP 3 against drug-persistent and stationary *S. aureus* cells revealed that CAP 3 at 8 μ M was able to combat persistent and stationary *S. aureus* bacteria with a >5-log reduction in CFU, whereas ampicillin was inactive (Fig. S2B). A mutant prevention assay (39) revealed that CAP 3 was active against higher CFU of *S. aureus*. CAP 3 at 8 μ M ($1 \times \text{MIC}_{99}$) was able to clear the bacterial growth even at 10^{12} CFU/ml, indicating its highly potent antimicrobial nature against persisters as well (Fig. S2C). In contrast, we observed a 4-fold increase in the MIC₉₉ of polymyxin B at 10^{10} and 10^{12} CFU/ml.

Similarly, *C. albicans* did not develop resistance against CAP 3, as we observed complete killing of *C. albicans* at 4 μ M for multiple generations whereas fluconazole treatments induced drug resistance in *C. albicans* over multiple treatments (see Fig. S3A at the above-mentioned URL). CAP 3 treatment at 4 μ M was able to clear the fungal growth even at higher CFU, whereas there was a multifold increase in the MIC₈₀ of fluconazole at 10^{10} and 10^{12} CFU/ml (Fig. S3B). Therefore, these studies confirmed the ability of CAP 3 to tackle drug-resistant and -persistent microorganisms without fail due to their ability to interact with bacterial and fungal membranes.

Disruption and prevention of *S. aureus* and *C. albicans* biofilms. Next, we tested the ability of CAP 3 to disrupt preformed *S. aureus* biofilms in a dose-dependent manner (40), where preformed thick biofilms were treated with different concentrations (8, 16, and 32 μ M) of CAP 3 for 24 h and processed for CFU analysis. Ciprofloxacin (CIPX; 32 μ M) was used as a positive control. There was an ~ 5 -log reduction in CFU upon treatment of CAP 3 at 32 μ M, confirming its ability to disrupt the bacterial biofilms similarly to ciprofloxacin (Fig. 3A). Similarly, treatment of preformed *C. albicans* biofilms with different doses of CAP 3 (8, 16, and 32 μ M) and fluconazole (FLU; 32 μ M) for 24 h confirmed a dose-dependent reduction in the fungal load, with an ~ 4 -log reduction in CFU at 32 μ M of CAP 3, similar to that with fluconazole (Fig. 3B).

The bactericidal nature of CAP 3 on preformed *S. aureus* biofilms was then confirmed by confocal laser scanning microscopy (CLSM) after SYTO 9-PI staining. CLS micrographs of untreated biofilms showed a thick green mass of viable *S. aureus* bacteria stained with SYTO 9 without any PI-stained dead bacteria (Fig. 3C). CAP 3 (32 μ M) treatment resulted in a significant decrease in green fluorescent cells and an increase of PI-stained red *S. aureus* bacteria, suggesting the disruption of the bacterial biofilms (Fig. 3C). Quantification of biofilm thickness confirmed an ~ 2 -fold decrease with CAP 3 treatment compared to that of untreated biofilms (Fig. 3D). Similarly, untreated *C. albicans* biofilms showed a thick green mass of biofilm stained with SYTO 9, confirming the *Candida albicans* cells were viable (Fig. 3E). In contrast, CAP 3-treated (32 μ M) cover glasses showed an increase in the number of PI-stained red *Candida albicans* cells and a significant decrease in green viable cells, confirming the fungicidal effect of CAP 3 on biofilms as well (Fig. 3E). There was an ~ 1.5 -fold reduction in biofilm thickness on CAP 3 treatment compared to that of untreated biofilms (Fig. 3F).

To test the ability of CAP 3 to prevent the formation of *S. aureus* biofilms, cover glasses were first coated (3 dips in 20 mg/ml of dichloromethane [DCM] solution of CAP 3) with CAP 3 as described in Materials and Methods and then incubated with *S. aureus* culture (10 μ l of 10^6 CFU/ml in 1 ml medium) for 24 h. Uncoated and dichloromethane

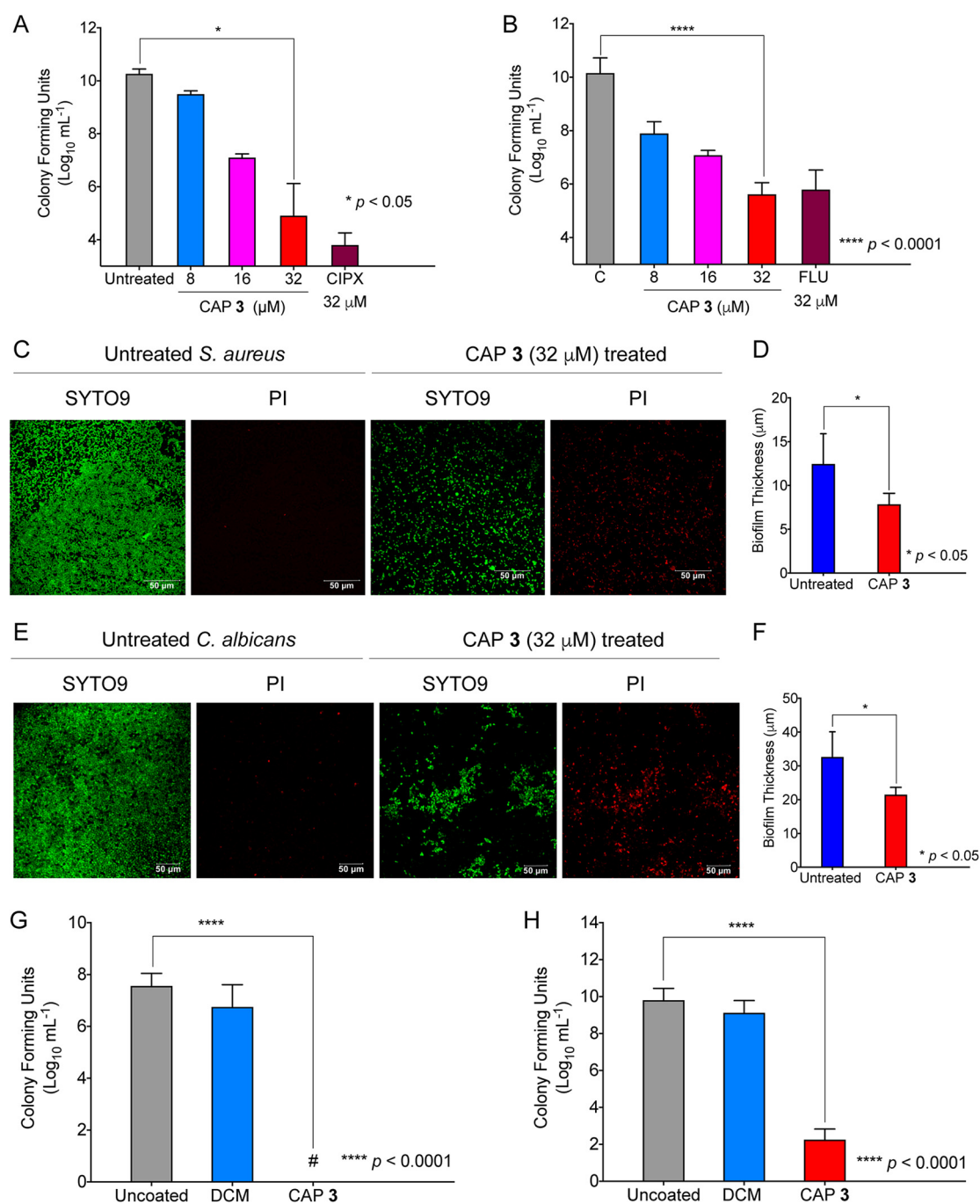


FIG 3 Quantifications of *S. aureus* (A) and *C. albicans* (B) by CFU assay after treatment of preformed single-species biofilms with different doses of CAP 3 (8, 16, and 32 μM) for 24 h confirm the ability of CAP 3 to degrade the biofilms. Ciprofloxacin (CIPX) (32 μM) was used as a control for *S. aureus* and fluconazole (FLU) (32 μM) was used as a control for *C. albicans*. Data are presented as means \pm SEMs from three biological replicates, and statistical analysis was performed by unpaired two-tailed Student's *t* tests. (C) SYTO 9-PI staining of untreated and CAP 3-treated (32 μM) *S. aureus* biofilms confirm the bactericidal effect of CAP 3 on biofilms, as we observed an increase in the number of red cells after CAP 3 treatment. (D) Quantification of untreated and CAP 3-treated (32 μM) *S. aureus* biofilms confirms an ~ 2 -fold reduction in thickness of biofilms after CAP 3 treatment. Data are presented as means \pm SDs from at least eight different images, and statistical analysis was performed by unpaired two-tailed Student's *t* test. (E) SYTO 9-PI staining of untreated and CAP 3-treated (32 μM) *C. albicans* biofilms confirm the fungicidal effect of CAP 3 on biofilms, as we observed an increase in the number of red cells after CAP 3 treatment. (F) Quantification of untreated and CAP 3-treated (32 μM) *C. albicans* biofilms confirms an >1.5 -fold reduction in the thickness of biofilms after CAP 3 treatment. Data are presented as means \pm SDs from at least eight different images, and statistical analysis was performed by unpaired two-tailed Student's *t* test. Quantifications of *S. aureus* (G) and *C. albicans* (H) biofilms on uncoated and DCM- and CAP 3-coated cover glasses (3 dips in 20 mg/ml of dichloromethane [DCM] solution of CAP 3) by CFU assays demonstrate the ability of the CAP 3 to prevent the formation of biofilms. Data are presented as means \pm SDs from three biological replicates, and statistical analysis was performed by unpaired two-tailed Student's *t* tests.

(DCM)-coated cover glasses were used as controls. CFU analysis after 24 h of incubation demonstrated growth of biofilms on uncoated and DCM-coated cover glasses (Fig. 3G). In contrast, there were no bacterial colonies on plates from CAP 3-coated cover glasses, thereby confirming its ability to prevent the formation of *S. aureus* biofilms (Fig. 3G). Incubation of uncoated and DCM- and CAP 3-coated cover glasses with *C. albicans* inoculum ($10\ \mu\text{l}$ of 10^6 CFU/ml in 1 ml medium) revealed a >6 -log reduction in adherence of cells on CAP 3-coated cover glasses compared to that on uncoated and DCM-coated cover glasses, thereby inhibiting the formation of *C. albicans* biofilms (Fig. 3H). These results clearly supported the ability of CAP 3 to degrade and prevent the formation of biofilms by Gram-positive bacteria and fungi.

Disruption and prevention of polymicrobial biofilms. We assessed the bactericidal and fungicidal effect of CAP 3 on polymicrobial biofilms formed by *S. aureus* and *C. albicans*. Polymicrobial biofilm formation was standardized under different conditions, and the most suitable conditions as mentioned in Materials and Methods was a combination of $100\ \mu\text{l}$ *C. albicans* of 10^6 CFU/ml and $50\ \mu\text{l}$ of *S. aureus* of 10^6 CFU/ml. Preformed polymicrobial biofilms were treated with different doses of CAP 3 (8, 16, and $32\ \mu\text{M}$) for 24 h and analyzed by CFU analysis. A combination of ciprofloxacin ($32\ \mu\text{M}$) and fluconazole ($32\ \mu\text{M}$) (CIPF) was used as a positive control. CFU analysis revealed ~ 4 - to 5-log reductions in CFU for both *S. aureus* and *C. albicans* with CAP 3 treatment at $32\ \mu\text{M}$ (Fig. 4A). Interestingly, CAP 3 treatment alone was found to be as effective as the combination of ciprofloxacin ($32\ \mu\text{M}$) and fluconazole ($32\ \mu\text{M}$) (CIPF). The ability of CAP 3-coated cover glasses to prevent the formation of polymicrobial biofilms was tested upon the incubation of the coverslips with coculture of *S. aureus* and *C. albicans*, as mentioned in Materials and Methods. CFU analysis confirmed that CAP 3-coated cover glasses induced an ~ 2 -log reduction in adherence of *S. aureus* and *C. albicans* compared to that on uncoated and DCM-coated cover glasses, thereby confirming its broad-spectrum antimicrobial activity (Fig. 4B). Similarly, treatment of preformed biofilms on catheters with CAP 3 ($32\ \mu\text{M}$) allowed 3- to 4-log reductions in *S. aureus* and *C. albicans* (see Fig. S4A posted at <https://rcb.res.in/upload/Revised%20SI%20PR%20MS.pdf>), and CAP 3-coated catheters (15 dips in 20 mg/ml of dichloromethane [DCM] solution of CAP 3) induced >2 -log reductions in adherence of *S. aureus* and *C. albicans*, whereas there was formation of a dense biofilm on uncoated and DCM-coated catheters (Fig. S4B).

For visualizing the efficacy of CAP 3 in degrading polymicrobial biofilms, we selected green fluorescent protein (GFP)-expressing *C. albicans* and mCitrine-expressing *S. aureus* for biofilm formation. We observed mature polymicrobial biofilms after 8 days of incubation, where a close adherence of both the species was seen clearly (Fig. 4C). Treatment of these polymicrobial biofilms with CAP 3 ($32\ \mu\text{M}$) for 24 h significantly reduced fluorescent *C. albicans* and *S. aureus* (Fig. 4D). SYTO 9-PI staining of polymicrobial biofilms using nonfluorescent *C. albicans* and *S. aureus* strains was performed to see the killing efficacy of CAP 3 on interspecies biofilms, which are denser and hence more challenging. While untreated biofilms had green fluorescent bacterial and fungal species (Fig. 4E), the CAP 3 ($32\ \mu\text{M}$) treatment induced a significant reduction of overall SYTO 9-stained green bacterial and fungal cells and an increased number of PI-positive red dead cells (Fig. 4F). Quantification of biofilm thickness showed that untreated polymicrobial biofilms form an $\sim 12\text{-}\mu\text{m}$ -thick biofilm, and CAP 3 ($32\ \mu\text{M}$) treatment for 24 h reduced the biofilm thickness to $\sim 3\ \mu\text{m}$ (Fig. 4G). These studies confirm the ability of CAP 3 to penetrate the tough extracellular polysaccharide matrix, causing a significant depletion of the biofilm biomass.

Effect of CAP 3 on biofilm architecture. To decipher the effect of CAP 3 on biofilm architecture, scanning electron microscopy (SEM) for *S. aureus*, *C. albicans*, and polymicrobial biofilms before and after 24 h treatment with CAP 3 was performed. Treatment of robust *S. aureus* biofilms embedded within a thick matrix with CAP 3 ($32\ \mu\text{M}$) showed the lethal effect (Fig. 5A). CAP 3 was able to penetrate the extracellular polysaccharide matrix and cause disruptions. Low-magnified images indicate a drastic

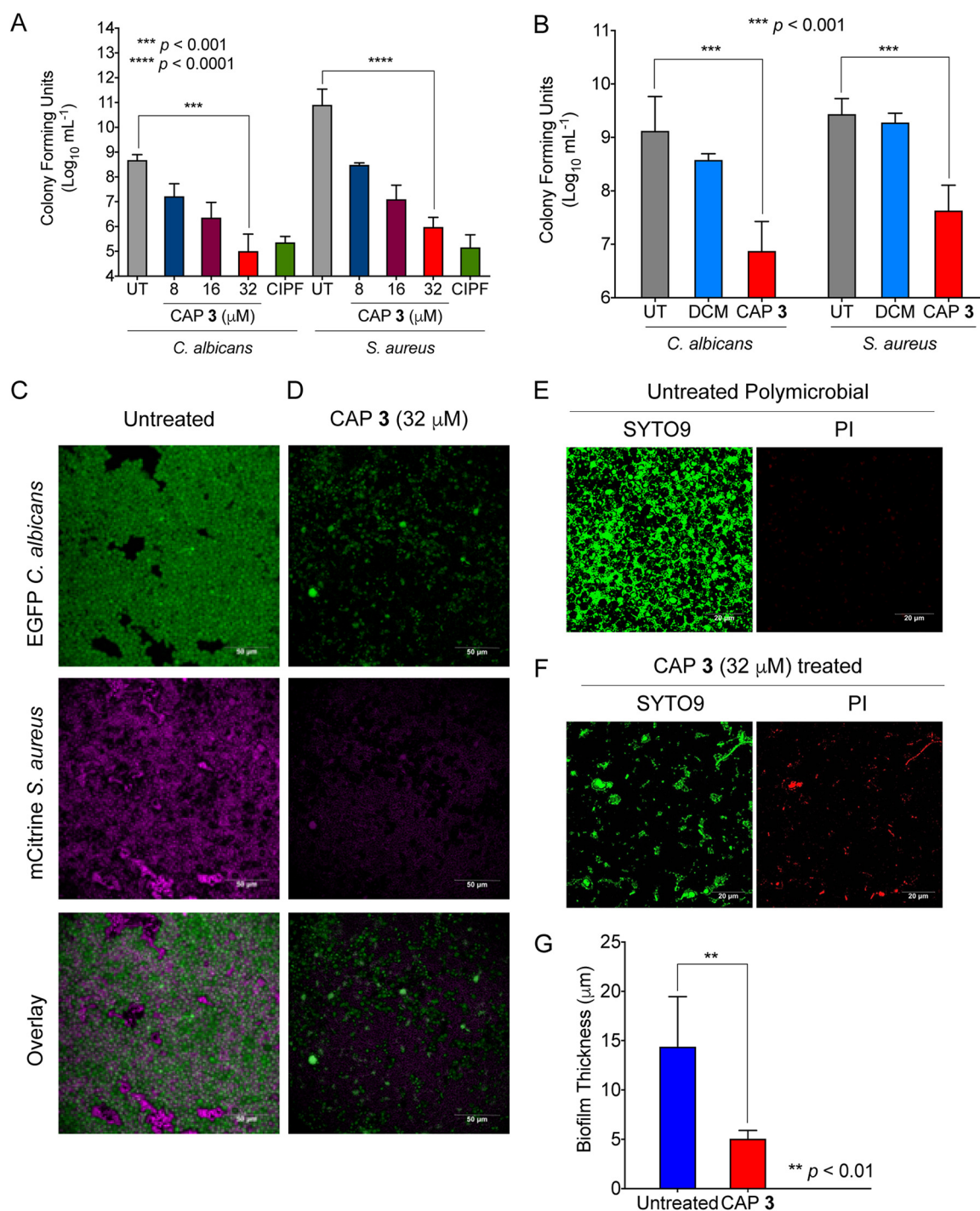


FIG 4 (A) Quantification of *S. aureus* and *C. albicans* by CFU assay after treatment of preformed polymicrobial biofilms with different doses of CAP 3 (8, 16, and 32 μM) for 24 h confirms the ability of CAP 3 to degrade the existing preformed biofilms similarly to CIPF, a combination of ciprofloxacin (32 μM) and fluconazole (32 μM). Data are presented as means ± SEMs from three biological replicates, and statistical analysis was performed by unpaired two-tailed Student's *t* tests. (B) Quantification of *S. aureus* and *C. albicans* adhered on uncoated and DCM- and CAP 3-coated cover glasses (3 dips in 20 mg/ml of dichloromethane [DCM] solution of CAP 3) by CFU assay reveals the ability of CAP 3 to prevent the formation of polymicrobial biofilms. Data are presented as means ± SEMs from three biological replicates, and statistical analysis was performed by unpaired two-tailed Student's *t* tests. (C) Confocal micrographs of untreated polymicrobial biofilms formed by mCitrine-*S. aureus* and EGFP-*C. albicans* show a thick biofilm mass. (D) Confocal micrographs of CAP 3-treated (32 μM) polymicrobial biofilms confirm bactericidal and fungicidal effects of CAP 3 on polymicrobial biofilms. Confocal micrographs of SYTO 9-PI stained untreated (E) and CAP 3-treated (32 μM) (F) polymicrobial biofilms confirm the ability of CAP 3 to have bactericidal and fungicidal effect on biofilms, as we observed an increase in the number of bacterial and fungal red cells after CAP 3 treatment. (G) Quantification of untreated and CAP 3-treated (32 μM) polymicrobial biofilms formed by mCitrine-*S. aureus* and EGFP-*C. albicans* confirms an ~3-fold reduction in thickness of biofilms on CAP 3 treatment. Data are presented as means ± SDs from at least eight different images, and statistical analysis was performed by unpaired two-tailed Student's *t* test.

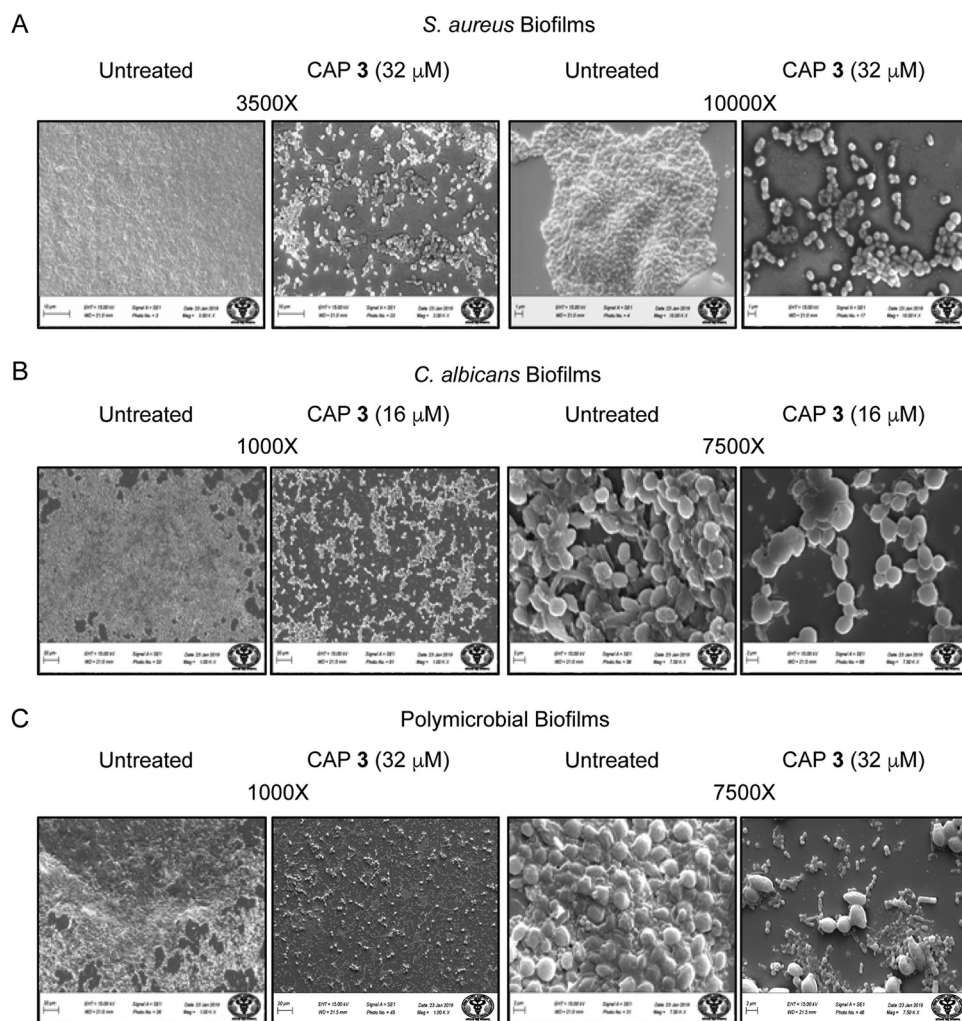


FIG 5 Scanning electron micrographs of untreated and CAP 3-treated *S. aureus* (A), *C. albicans* (B), and polymicrobial (C) biofilms. Lower and higher magnification images clearly indicate the degradation of biofilm after CAP 3 treatment. Numbers above panels indicate the magnification.

overall biofilm reduction, while at higher magnification, the punctured cells can clearly be seen. *C. albicans* forms a highly dense biofilm, with its interspersed hyphal forms indicating that the biofilm reached a stage between intermediate and mature form (Fig. 5B). The presence of a thick extracellular polysaccharide matrix surrounding the cells was seen in the untreated biofilm. Upon CAP 3 treatment (16 μ M), the disruption of extracellular polysaccharide matrix was clearly evident, as cells were now devoid of clusters (Fig. 5B). Compared to the individual biofilms, the untreated polymicrobial biofilm showed a different phenotype with an expected much thicker extracellular polysaccharide matrix, where smaller *S. aureus* cells were found in chains around the *Candida albicans* cells (Fig. 5C). There was no presence of any dense hyphae in polymicrobial biofilms with CAP 3 treatment (32 μ M), and there were significant reductions in overall biofilm thickness and density, unlike in untreated biofilms. These results clearly confirm that CAP 3 can successfully degrade single-species and polymicrobial biofilms.

Antimicrobial activity of CAP 3 against wound infections. In the first experiment, BALB/c mice having wounds on their skin were infected with *S. aureus* and randomized into three groups ($n = 3/\text{group}$). Group 1 mice were treated with saline thrice a day, group 2 mice were treated with neomycin (40 mg/kg of body weight, thrice a day), and mice in group 3 were treated with CAP 3 (40 mg/kg, thrice a day) (Fig. 6A). Quantifi-

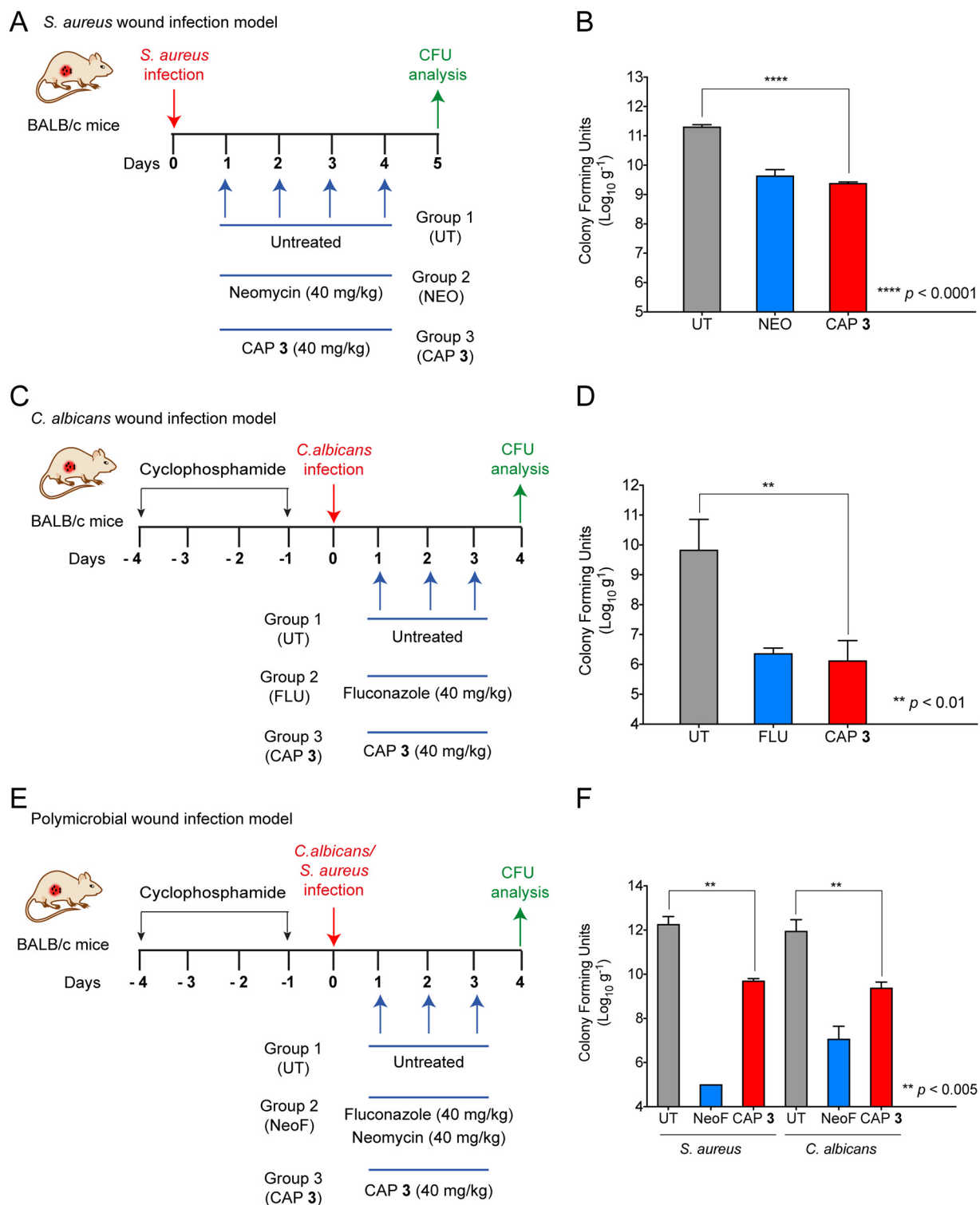


FIG 6 (A) Schematic presentation of the *S. aureus* wound infection assay in BALB/c mice, where infected mice ($n = 3/\text{group}$) were treated for three times/day for 4 days with CAP 3, and neomycin and bacterial load was quantified by plating. (B) Quantification of the bacterial load confirms the ability of the CAP 3 to significantly clear the bacterial load. (C) Schematic presentation of the *C. albicans* neutropenic wound infection model, where two doses of cyclophosphamide were used to obtain neutropenic mice. Mice were infected with *C. albicans* and randomized into three groups ($n = 3/\text{group}$). One group was left untreated. Two groups were treated three times per day for 3 days with CAP 3 (40 mg/kg) or fluconazole (40 mg/kg). Fungal load was quantified by plating. (D) Quantification of *C. albicans* from wound infections confirms the ability of CAP 3 to clear the fungal infections from wounds. (E) Schematic presentation of the polymicrobial wound infection model, where mice ($n = 3/\text{group}$) were made neutropenic with cyclophosphamide followed by infection with combination of *S. aureus* and *C. albicans*. One group of mice was left untreated, a second group of mice (NeoF) was treated with a combination of neomycin (40 mg/kg) and fluconazole (40 mg/kg), and a third group was treated with CAP 3 (40 mg/kg). All treatments were given three times a day for 3 days. Bacterial and fungal load was quantified by CFU assay after 3 days.

(Continued on next page)

cation by CFU analysis on day 5 indicated a >2 -log reduction in bacterial burden after CAP 3 treatment, similar to that with neomycin (Fig. 6B), thereby confirming the ability of CAP 3 to clear the *S. aureus* wound infections.

For the *C. albicans*-mediated wound infection model, mice were given two doses of cyclophosphamide on day -4 (150 mg/kg) and -1 (100 mg/kg) to make them neutropenic followed by wound infection on day 0 (Fig. 6C) (41). Infected mice were randomized into three groups ($n = 3$ /group), where group 1 mice were left untreated, group 2 mice were treated with fluconazole (40 mg/kg, thrice a day), and group 3 was treated with CAP 3 (40 mg/kg, thrice a day) (Fig. 6C). CFU quantification on day 4 revealed a >3 -log reduction in fungal growth, confirming the fungicidal effect of CAP 3 in wound infections (Fig. 6D).

In the polymicrobial wound infection model, neutropenic mice were infected with *S. aureus* and *C. albicans* after creating wounds on their skin (Fig. 6E). Mice were randomized into three groups ($n = 3$ /group), where group 1 mice were left untreated, group 2 was treated with a combination of neomycin (40 mg/kg, thrice a day) and fluconazole (40 mg/kg, thrice a day), and group 3 was treated with CAP 3 (40 mg/kg, thrice a day) (Fig. 6E). Quantification of the microbial burden on day 4 by CFU analysis showed ~ 2 -log decreases in both *S. aureus* and *C. albicans* colonies with CAP 3 treatment (Fig. 6F). These results confirm that CAP 3 is a broad-spectrum antimicrobial and can clear polymicrobial wound infections.

Prevention of biofilms in catheter infections using CAP 3. For an effective noninvasive quantification of bacterial load on catheters in mice, we used a bioluminescent strain of *S. aureus* (Xen 36) that shows bioluminescence without the application of any substrate (42). To test the effect of CAP 3-coated catheters on *S. aureus* biofilm formation, BALB/c mice were randomized into three groups ($n = 3$ /group), and uncoated and DCM- and CAP 3-coated catheters were inserted subcutaneously in three different groups of mice followed by infection with Xen 36 (Fig. 7A). On day 6, bioluminescence quantification of the bacteria was performed using an *in vivo* imaging system (IVIS). Whole-body images showed a significantly reduced bioluminescence from mice having CAP 3-coated catheters compared to that in mice with uncoated and DCM-coated catheters (Fig. 7B). Quantification of the bioluminescence further verified the ability of CAP 3-coated catheters to inhibit biofilm formation (Fig. 7C). CFU analysis of excised catheters showed an ~ 3 -log reduction in bacterial load from CAP 3-coated catheters compared to that from uncoated and DCM-coated catheters, thereby confirming the antifouling and bactericidal effect of CAP 3-coated catheters in mice (Fig. 7D).

Efficacy of CAP 3-coated catheters to prevent the formation of *C. albicans* biofilm was tested using bioluminescent *C. albicans* strain pACT1:*luc*_{OPT} (3B10). This strain was engineered using a synthetic luciferase gene completely adapted for high expression in *C. albicans* and shows bioluminescence after the addition of D-luciferin substrate (43). Neutropenic mice ($n = 4$ /group) having uncoated and DCM- and CAP 3-coated catheters were infected with pACT1:*luc*_{OPT} (3B10), and biofilm growth was quantified by bioluminescence imaging (Fig. 7E). Mice bearing uncoated and DCM-coated catheters showed strong bioluminescence on day 5 due to the formation of *C. albicans* biofilm on the catheters (Fig. 7F). In contrast, a significant reduction in bioluminescence from mice bearing CAP 3-coated catheters confirmed the ability of CAP 3 to prevent biofilm formation (Fig. 7F and G). CFU analysis confirmed its prevention effect, as there was an ~ 5 -log reduction in the number of colonies grown on CAP 3-coated catheters compared to those on uncoated and DCM-coated catheters (Fig. 7H).

To validate the effect of CAP 3 in preventing polymicrobial biofilm formation (44), uncoated and DCM- and CAP 3-coated catheters were inserted subcutaneously in three

FIG 6 Legend (Continued)

(F) CFU quantification after different treatments confirms the bactericidal and fungicidal effect of CAP 3 similarly to that with the combination of neomycin and fluconazole (NeoF). Data are presented as means \pm SDs, and statistical analysis was performed by unpaired two-tailed Student's *t* tests.

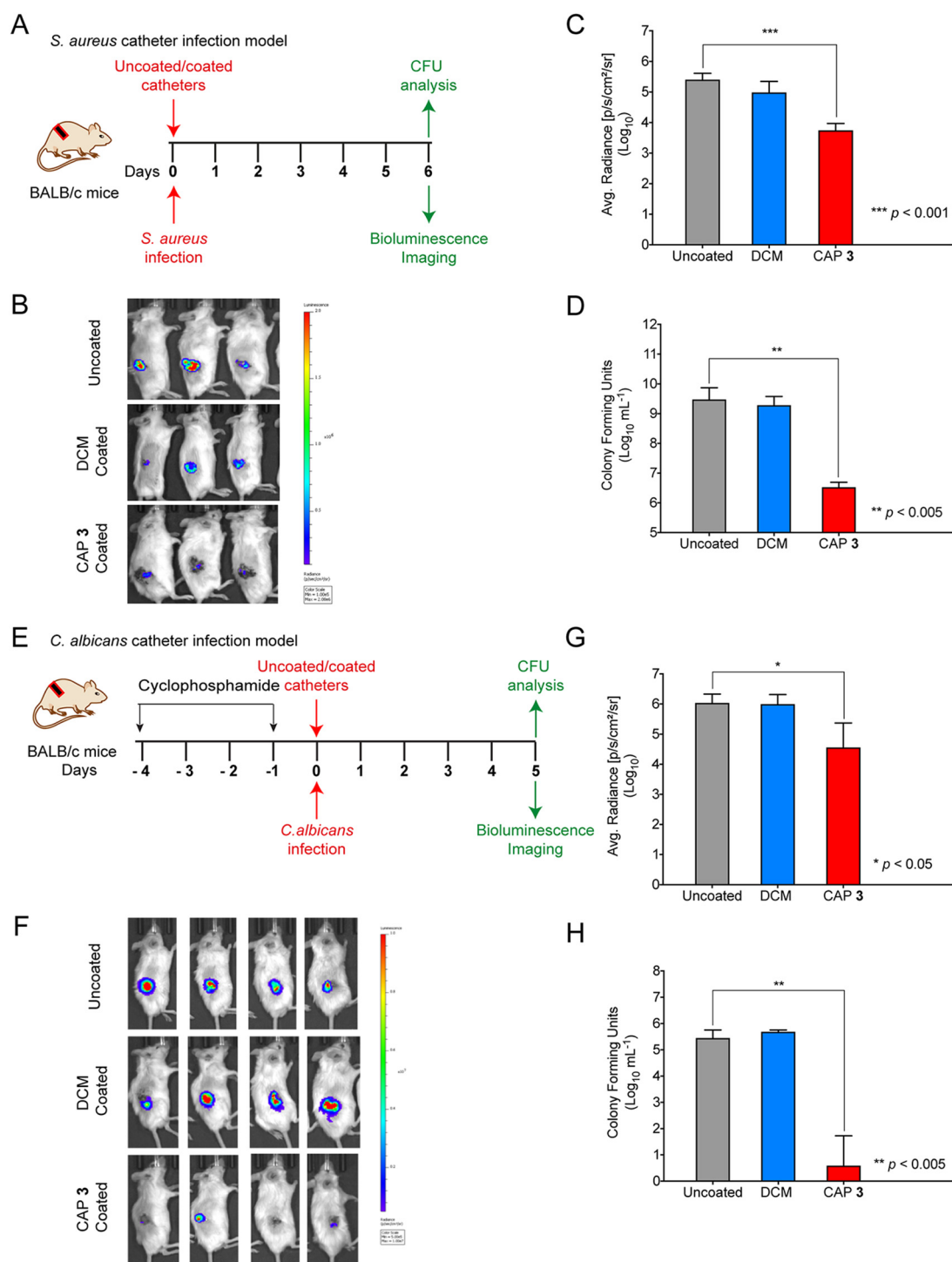


FIG 7 (A) Schematic presentation of *S. aureus* catheter infection model, where uncoated and DCM- and CAP 3-coated catheters (15 dips in 20 mg/ml of dichloromethane [DCM] solution of CAP 3) were inserted subcutaneously into mice from three groups of mice ($n = 3/\text{group}$) followed by infection with bioluminescent *S. aureus* (Xen 36). Bioluminescence imaging was performed on day 6 followed by CFU quantification from isolated catheters. Whole-body bioluminescence (B) and its quantification (C) from mice with uncoated and DCM- and CAP 3-coated infected catheters show a significant reduction in bioluminescence in the case of CAP 3-coated catheters. (D) CFU quantification from excised uncoated and DCM- and CAP 3-coated catheters on day 6 confirms an >3 -log reduction in bacterial load from CAP 3-coated catheters compared to that from uncoated catheters. (E) Schematic presentation of *C. albicans* catheter infection assay, where uncoated and DCM- and CAP 3-coated catheters were inserted subcutaneously into neutropenic mice in three groups ($n = 4/\text{group}$) followed by infection with bioluminescent *C. albicans*. Bioluminescence imaging was performed on day 5 followed by CFU quantification. Whole-body bioluminescence (F) and quantification of bioluminescence (G) from mice with uncoated and DCM- and CAP 3-coated infected catheters after D-luciferin injection show a significant reduction of bioluminescence in the case of CAP 3-coated catheters. (H) CFU quantification from

(Continued on next page)

different groups of neutropenic BALB/c mice ($n \geq 3/\text{group}$). This was followed by infection using a combination of bioluminescent *S. aureus* (Xen 36) and *C. albicans* pACT1:*luc*_{OPT} (3B10) (Fig. 8A). Xen 36 shows bioluminescence without application of any substrate at 489 nm, and *C. albicans* shows bioluminescence only after reaction with D-luciferin at 612 nm. On day 4, whole-body bioluminescence imaging was performed to quantify the microbial load on catheters followed by spectral unmixing as described in Materials and Methods. The bioluminescence of *S. aureus* revealed a significant reduction in bacterial load in mice bearing CAP 3-coated catheters (Fig. 8B top and Fig. 8C) that was further confirmed by its quantification (Fig. 8C). Bioluminescent images and quantitation also validated the significant reduction of fungal load in mice with CAP 3-coated catheters (Fig. 8B middle and Fig. 8C). Bioluminescent images obtained after spectral unmixing of *S. aureus* (green) and *C. albicans* (red) bioluminescence are presented as an overlay in Fig. 8B (bottom) that confirm the significant reductions in bacterial and fungal loads in mice with CAP 3-coated catheters. CFU analysis further denoted the significant reduction in *S. aureus* and *C. albicans* loads at the infected site, thereby confirming the ability of CAP 3-coated catheters to prevent polymicrobial infections (Fig. 8D). These results, therefore, validated the ability of CAP 3 to prevent the formation of polymicrobial biofilms in murine models.

Conclusions. In summary, we screened 20 cholic acid-peptide conjugates (CAPs) for their antimicrobial activity against different Gram-positive bacterial and fungal strains. Valine-glycine-derived CAP 3 was most active with a broad-spectrum antimicrobial activity and successfully cleared drug-resistant and -persistent as well as stationary microorganisms. Mechanistic investigations including TEM studies confirmed that CAP 3 interacted with microbial cell membranes, followed by membrane disruptions. CAP 3 can degrade the preformed *S. aureus* and *C. albicans* biofilms and can also prevent the formation of biofilms on CAP 3-coated materials. Interestingly, CAP 3 treatment cleared the interkingdom polymicrobial biofilms formed by *S. aureus* and *C. albicans*, and CAP 3-coated catheters did not allow the formation of these polymicrobial biofilms. We further confirmed the broad-spectrum antimicrobial effect of CAP 3 in wound and catheter infection models in mice, where spectral unmixing data clearly showed the efficacy of CAP 3 in preventing dual species infections. Therefore, for the first time, this study reveals the broad-spectrum antimicrobial effect of CAPs and their ability to degrade as well as prevent the growth of interkingdom polymicrobial biofilms. This study will help in the future design of effective broad-spectrum antimicrobials for targeting polymicrobial biofilms.

MATERIALS AND METHODS

Materials. Luria-Bertani (LB) broth (M1245), LB agar (M1151), tryptone soy broth (TSB; M011), nutrient broth (M002), bacteriological agar (PCT0901), yeast extract-peptone-dextrose (YPD) (M1363) broth, ampicillin sodium salt (CMS645), chloramphenicol (CMS218), trypsin-EDTA (TCL007), and fluconazole (CMS8387) were procured from HiMedia. Ciprofloxacin (17850) was from Fluka. *N*-Phenyl-1-naphthylamine (104043), kanamycin B sulfate (B5264), propidium iodide (P1470), and neomycin sulfate (PHR1491) were purchased from Sigma. Dermabond, a topical skin adhesive, was obtained from Ethicon, USA. LIVE/DEAD BacLight bacterial viability kit was purchased from Molecular Probes, Thermo Fisher Scientific, USA. Luciferin substrate, XenoLight D-luciferin potassium salt (122799), and the Xen 36 bioluminescent *S. aureus* (ATCC 49525) strain were purchased from Perkin Elmer, USA. Plasmids mCitrine-pBAD (plasmid 54723) and pCypet-His (plasmid 14030) were obtained from Addgene (45). *S. aureus* (MTCC 737), *S. pneumoniae* (MTCC 1936), and *B. subtilis* (MTCC 441) were obtained from MTCC. *C. albicans* (SC 5134), *C. tropicalis* (ATCC 756), and *C. kefyr* (ATCC 2512) were obtained from MTCC or ATCC. Fluorescent *S. aureus* stains were prepared using plasmid mCitrine-pBAD (plasmid 54723) and pCypet-His (plasmid 14030) by simple bacterial transformation. *S. aureus* harboring mCitrine-pBAD was used for polymicrobial microscopy studies, and *S. aureus* harboring pCypet-His (containing a chloramphenicol selection marker) was used for CFU analysis of polymicrobial biofilms. Enhanced GFP (EGFP)-expressing *Candida albicans* BWP17 strain was a kind gift from Alistair J. P. Brown, University of Aberdeen, UK, and Sudha Komath, School of Life Sciences, Jawaharlal Nehru University, New Delhi, India. Bioluminescent *Candida* strain

FIG 7 Legend (Continued)

excised uncoated and DCM- and CAP 3-coated catheters on day 5 confirms a >4 -log reduction in fungal load from CAP 3-coated catheters compared to that from uncoated catheters. Data are presented as means \pm SDs, and statistical analysis was performed by unpaired two-tailed Student's *t* tests.

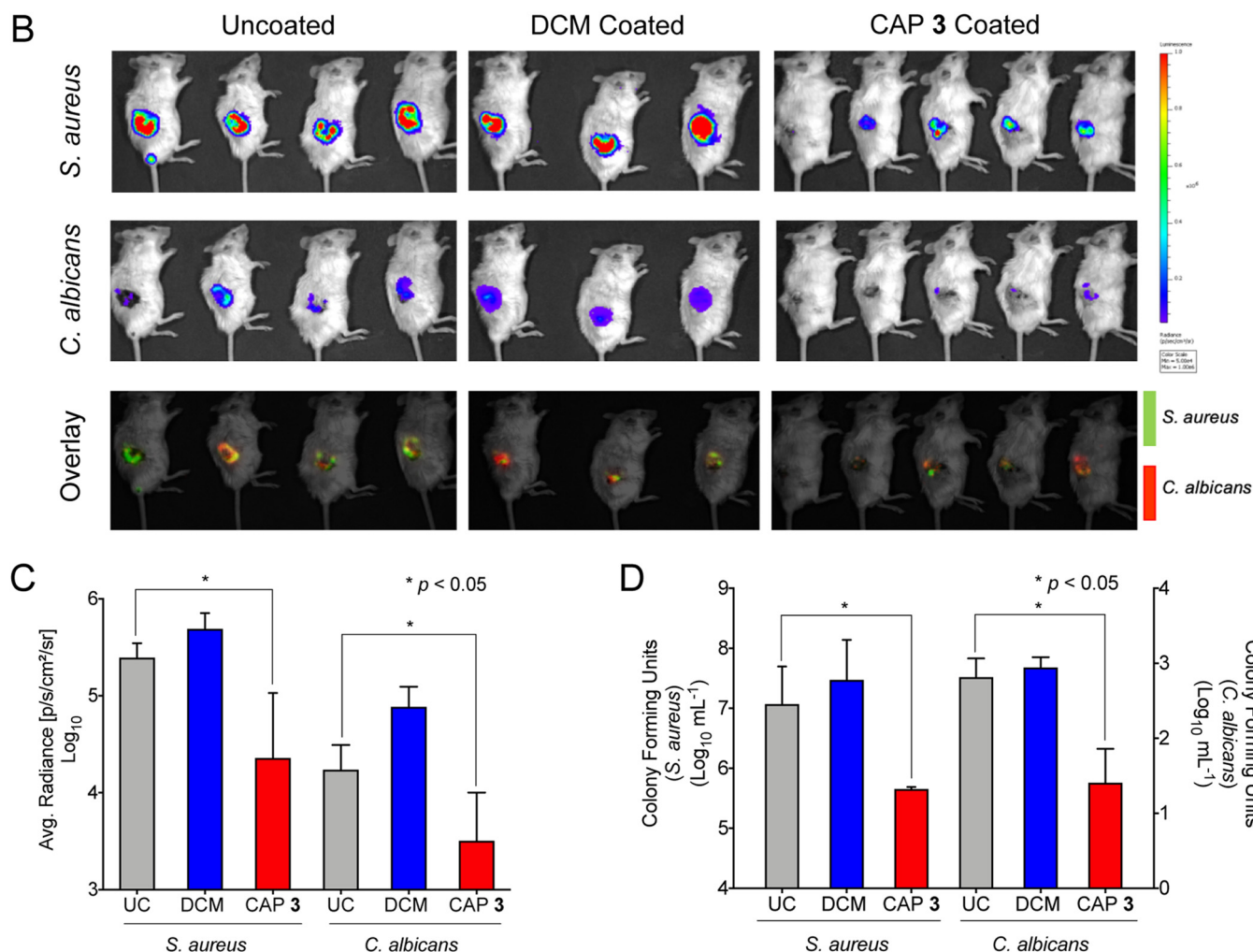
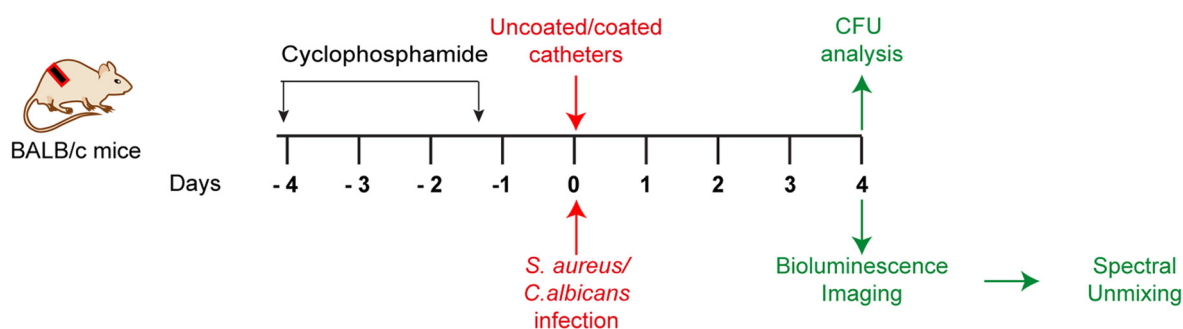
A Polymicrobial catheter infection model

FIG 8 (A) Schematic presentation of the polymicrobial catheter infection model, where three groups of mice ($n \geq 3$ /group) were made neutropenic by cyclophosphamide injections, and uncoated and DCM- and CAP 3-coated catheters (15 dips in 20 mg/ml of dichloromethane [DCM] solution of CAP 3) were inserted subcutaneously followed by *S. aureus* and *C. albicans* infection. Bioluminescence imaging was performed on day 4 followed by CFU quantification. (B) Whole-body bioluminescence images of mice after injections of p-luciferin and spectral unmixing show effects of CAP 3 on bacterial (top) and fungal (middle) infection loads. (Bottom) Overlay confirms the ability of CAP 3-coated catheters to prevent the formation of polymicrobial biofilms. (C) Quantification of bioluminescence after p-luciferin injections and spectral unmixing from mice with uncoated and DCM- and CAP 3-coated catheters shows a significant reduction in bioluminescence in the case of CAP 3-coated catheters. (D) CFUs quantified from excised uncoated and DCM- and CAP 3-coated catheters on day 4 confirm the significant reduction in bacterial and fungal loads from CAP 3-coated catheters. Data are presented as means \pm SDs, and statistical analysis was performed by unpaired two-tailed Student's *t* tests.

pACT1:*luc*_{OPT} (3B10) was a kind gift from Matthias Brock, University of Nottingham (UK), and the Hans-Knoll-Institute Jena (Germany).

Microbial culture and antibacterial and antifungal activity assays. Bacteria were cultured using LB broth, and *Candida* strains were cultured using yeast extract-peptone-dextrose (YPD) broth with

ampicillin (100 $\mu\text{g/ml}$). Antibacterial and antifungal activities were tested using the broth dilution method as described in the Clinical and Laboratory Standards Institute (CLSI) susceptibility testing guidelines (31, 32). Amphiphiles were serially (2-fold) diluted from 256 μM to 0.5 μM (100 μl) in a 96-well plate, and bacterial/fungal cultures were then added (100 μl) with respective optical density (OD) values (0.1 corresponding to 10^5 CFU/ml for bacteria and to 10^6 CFU/ml for fungal strains) (31, 32). Bacterial plates were incubated at 37°C for 18 h and fungal plates at 30°C for 48 h, and the OD was measured at 600 nm using a Spectramax M5 multimode microplate reader (Molecular Devices, Sunnyvale, CA, USA). Polymyxin B and fluconazole were used for the positive controls, while pure culture broth was taken as the sterility control. Antibacterial activities are presented as $\text{MIC}_{99.5}$ for bacteria and $\text{MIC}_{80.5}$ for fungi.

Bactericidal and fungicidal time kinetic studies. Bactericidal and fungicidal effects of amphiphiles against *S. aureus* or *C. albicans* were determined using previously published protocols (46, 47). *S. aureus* or *C. albicans* culture was grown until log phase and centrifuged at 5,000 rpm for 10 min. Cells were resuspended in fresh LB (or YPD for *C. albicans*) broth, and the OD was adjusted to 0.1. Bacterial suspensions were treated with CAP 3 at 16 and 32 μM (or 8 and 16 μM for *C. albicans*). At different time points, untreated and treated suspensions were taken out, serially diluted, and plated on LB agar plates (or YPD plates for *C. albicans*). The plates were incubated at 37°C for 16 to 18 h (or at 30°C for 48 h), and colonies were counted and expressed as \log_{10} CFU per milliliter as a function of time. Data are represented as means \pm standard errors of the means (SEMs) from three biological replicates.

Membrane potential fluorescence assay. We investigated the changes in membrane potential of *S. aureus* bacteria after treatment with amphiphiles by using DiSC₂(5)-based fluorescence assay (33, 48). *S. aureus* cells were grown until log phase and harvested. The culture was centrifuged at 5,000 rpm for 10 min, resuspended in phosphate-buffered saline (PBS; with 1% glucose), and the OD was adjusted to 0.1 corresponding to 10^5 CFU/ml. DiSC₂(5) (final concentration 100 μM) was added to the culture and incubated at 37°C. Every 10 min, fluorescence at an excitation wavelength (λ_{ex}) of 637 nm and emission wavelength (λ_{em}) at 670 nm was measured, and KCl (100 mM final concentration) was added to help stabilize the membrane potential. Once the fluorescence values reached saturation, the culture was treated with CAP 3 and polymyxin B at 32 μM (four technical replicates each) and incubated at 37°C for 15 min. Later, treated suspensions were transferred to 96-well plates and fluorescence was measured for 80 min using a Spectramax M5 multimode microplate reader (Molecular Devices, Sunnyvale, CA, USA). The assay was conducted in three biological replicates, and data are presented as means \pm SEMs from three biological replicates.

NPN-based membrane permeabilization assay. The effect of amphiphiles on the permeabilization of fungal membranes of *C. albicans* was studied using *N*-phenyl-1-naphthylamine-based fluorescence assay (36). Log-phase fungal cultures were harvested and resuspended in PBS (with 1% glucose) with an OD corresponding to 10^5 CFU/ml. *N*-Phenyl-1-naphthylamine (NPN) solution with a final concentration of 10 μM was added to the cells and incubated for 15 min at 37°C. The fluorescence of cells was measured at intervals of 10 min until saturation was attained. NPN-labeled cells were then treated with CAP 3 at 8, 16, and 32 μM with three technical replicates each. The untreated and treated suspensions were kept at 37°C for 30 min, and fluorescence was measured for 20 with λ_{ex} of 350 nm and λ_{em} at 420 nm using a Spectramax M5 multimode microplate reader (Molecular Devices, Sunnyvale, CA, USA). The experiment was conducted in three biological replicates, and the data are presented as means \pm SEMs from three biological replicates.

Propidium iodide uptake assay. Membrane perturbations of *S. aureus* and *C. albicans* by amphiphiles were studied using a propidium iodide uptake assay (49). Cells of both *S. aureus* and *C. albicans* were then treated with CAP 3 at respective 1 \times , 2 \times , and 4 \times $\text{MIC}_{99}/\text{MIC}_{80}$ values for 30 and 60 min each (8, 16, and 32 μM for *S. aureus* and 4, 8, and 16 μM for *C. albicans*). After each time point, treated cells were stained with propidium iodide (PI) (10 $\mu\text{g/ml}$) and incubated at 37°C for 15 min followed by washing with PBS. Washed and resuspended cells were analyzed by flow cytometry using BD FACSVerser flow cytometer (BD Biosciences, San Jose, CA) under the propidium iodide channel. Populations of PI-positive cells were noted, and data were expressed as mean \pm SEMs from three biological replicates for both *S. aureus* and *C. albicans*.

Biofilm degradation assays. (i) *S. aureus* biofilm degradation assay. We tested the antimicrobial activity of amphiphile against *S. aureus* biofilms using a modified version of the published protocol (50). An overnight-grown culture of *S. aureus* was used to inoculate TSB for biofilm formation. Around 10 to 12 heat-sterilized cover glasses (~ 22 mm in diameter) or autoclaved catheters (~ 0.5 cm) were dipped in TSB (10 ml) in each petri plate containing *S. aureus* inoculum (10 μl of 10^6 CFU/ml) and incubated at 37°C. After 24 h, culture medium was replenished, and a dense biofilm was observed after 48 h. For the degradation assay, the preformed biofilms were treated with CAP 3 at different concentrations (8, 16, and 32 μM) for 24 h. Ciprofloxacin (CIPX) (32 μM) was used as the control. Biofilms were then treated with trypsin-EDTA (100 μl) for 15 min, and suspensions were serially diluted and plated on LB agar plates. Plates were incubated at 37°C for 24 h and bacterial colonies were counted and expressed as \log_{10} CFU per milliliter. The values are presented as means \pm SEMs from three biological replicates.

(ii) *C. albicans* biofilm degradation assay. For the *C. albicans* biofilm degradation assay (51), an overnight-grown culture of *C. albicans* in YPD broth with ampicillin (100 $\mu\text{g/ml}$) was used for inoculation. Around 10 to 12 heat-sterilized cover glasses (~ 22 mm in diameter) or autoclaved catheters (~ 0.5 cm) were first submerged in sterilized Spider medium (1% nutrient broth, 1% mannitol, 0.2% potassium hydrogen phosphate) containing the inoculum of *C. albicans* (10 μl of 10^6 CFU/ml) for 10 to 12 h at 37°C to ensure the adherence of fungal cells. Spider medium was then replaced with YPD broth (10 ml) containing ampicillin (100 $\mu\text{g/ml}$), and biofilms were incubated at 37°C for 7 days under static conditions. Medium was replenished every 24 h to maintain the nutrient balance and remove planktonic fungal cells,

with careful monitoring of biofilm progression under a microscope. For the degradation assay, the biofilms were treated with CAP 3 at concentrations of 8, 16, and 32 μM for 24 h. Fluconazole (32 μM) was used as a positive control. Biofilms were then trypsinized by adding 100 μl trypsin-EDTA solution for 15 min followed by serial dilutions of the suspensions and plating on YPD-ampicillin agar plates. Plates were incubated at 30°C for 48 h, fungal colonies were counted, and data are presented as means \pm SEMs from three biological replicates.

(iii) Polymicrobial biofilm degradation assay. We modified the previously published protocol for the preparation of polymicrobial biofilms (52). We incubated the cover glasses or catheters with *C. albicans* (100 μl of 10^6 CFU/ml) in Spider medium (10 ml) for 10 to 12 h at 30°C in a petri plate, and the medium was replaced with YPD broth (10 ml) and incubated at 37°C. After 24 h, we added the inoculum of pCypet-His-expressing *S. aureus* (50 μl of 10^6 CFU/ml) with ampicillin (100 $\mu\text{g/ml}$). The medium was then replenished with a 1:1 mixture of YPD and TSB (5 ml each) every 24 h for 7 days to ensure the formation of a thick biofilm. For the degradation assay, the cover glasses or catheters were immersed in 12-well plates and washed with PBS in order to remove any unbound planktonic species. Biofilms were then treated with different concentrations of CAP 3 (8, 16, and 32 μM) for 24 h at 37°C. Biofilms were then trypsinized as mentioned above, and the suspensions were serially diluted and plated simultaneously on LB-chloramphenicol agar plates and YPD-ampicillin agar plates. Plates were incubated at 37°C for 1 day for bacterial colonies and 30°C for 48 h for the appearance of fungal colonies. The degradation assay was carried out in three biological replicates, and data are presented as means \pm SEMs from three biological replicates.

Biofilm prevention assays. (i) Coating of cover glasses and catheters and quantification. Cover glasses (~22 mm diameter) and catheters were coated with dichloromethane (DCM) and CAP 3, where catheters were dipped for 15 times in DCM or DCM solution of CAP 3 (20 mg/ml) and dried. Uniformly coated cover glasses were obtained only after 3 dips of CAP 3.

(ii) *S. aureus* biofilm prevention assay. For the *S. aureus* biofilm prevention assay (53), the uncoated and coated catheters were placed in 24-well culture plates (1 per well, 3 technical replicates) containing LB broth (1 ml) inoculated with 10 μl of 10^6 CFU/ml inoculum of *S. aureus*. The plate was incubated at 37°C under stationary conditions, and after every 24 h, the culture medium was replenished. After 72 h, the medium was removed and catheters were gently washed in PBS (1 ml). Catheters were vortexed in PBS (1 ml) for 15 min to pull down the adhered bacteria in suspension. Bacterial suspensions were then plated on the LB agar plates and incubated at 37°C, and bacterial colonies were counted after 24 h. The data are presented as means \pm SEMs from three biological replicates.

(iii) *C. albicans* biofilm prevention assay. For the *C. albicans* biofilm prevention assay (54), the uncoated and coated cover glasses as well as catheters (1 per well, 3 technical replicates) were placed in 24-well culture plates and incubated in Spider medium containing 10 μl of *C. albicans* inoculum (10^6 CFU/ml) for 10 to 12 h to ensure the adherence of fungal cells to the surface. The medium was then replaced with YPD broth containing ampicillin (100 $\mu\text{g/ml}$). The plates were incubated at 37°C under stationary conditions, and the medium was changed every 24 h for nutrient balance and the removal of planktonic fungal cells. After 7 days, the medium was removed and cover glasses/catheters were gently washed in PBS (1 ml) followed by vortexing of catheters in PBS (1 ml) for 15 min. Serial dilutions of the suspension were then plated on the YPD-ampicillin agar plates and incubated at 30°C, and colonies were counted after 48 h. Data are presented as means \pm SEMs from three biological replicates.

(iv) Polymicrobial biofilm prevention assay. For the polymicrobial biofilm prevention assay (52), cobiofilms were prepared by incubating the cover glasses or catheters in 24-well culture plates (1 per well, 3 technical replicates) with *C. albicans* (100 μl of 10^6 CFU/ml) in Spider medium (10 ml) for 12 h. Spider medium was then replaced with YPD broth (10 ml) and incubated at 37°C. After 24 h, an inoculum of pCypet-expressing *S. aureus* (50 μl of 10^6 CFU/ml) was added after ensuring the adherence of *Candida* on the surfaces. The medium was then replenished with a 1:1 mixture of YPD and TSB (5 ml each) every 24 h for 7 days to ensure the formation of a thick biofilm. Biofilms were then trypsinized (100 μl trypsin-EDTA solution) for 15 to 20 min, and suspensions were plated on LB-chloramphenicol agar plates for *S. aureus* and YPD-ampicillin agar plates for *C. albicans*. Plates were incubated at 37°C for 1 day for growth of bacterial colonies and 30°C for 48 h for fungal colonies. The data are presented as means \pm SEMs from three biological replicates.

LIVE/DEAD staining. We used a LIVE/DEAD BacLight bacterial viability kit to investigate the live and dead cells in planktonic and biofilms after treatment with the amphiphile (55). Planktonic samples (log-phase cultures) of *C. albicans* (10^6 CFU/ml) as well as *S. aureus* (10^5 CFU/ml) were treated with CAP 3 at 8 μM (for *S. aureus*) and 4 μM (for *C. albicans*) for 6 h. The untreated and treated cultures were centrifuged (5,000 rpm for 10 min) and washed with PBS (1 ml). The two components of LIVE/DEAD BacLight bacterial viability kit, SYTO 9 and propidium iodide (PI), were mixed in a 1:1 (vol/vol) ratio. The dye mixture (1 μl) was then added to the culture (1 ml) and incubated at 37°C for 20 min. Cultures were then washed twice with PBS (1 ml) and fixed with 4% paraformaldehyde (PFA; 100 μl) for 30 min at 4°C followed by two washings with PBS (1 ml). Culture (10 μl) was then put on glass slides and covered with cover glass. After sealing the dried cover glasses with a transparent nail enamel, the slides were observed under an inverted confocal microscope (Leica TCS SP8; Leica, Germany) under a 63 \times oil objective in fluorescein isothiocyanate (FITC) (for SYTO 9, green) and tetramethyl rhodamine isocyanate (TRITC) (for PI, red) channels.

Similarly, untreated and treated biofilms of *C. albicans* (at 16 μM), *S. aureus* (at 32 μM), and polymicrobial cultures (at 32 μM) were washed and immersed in saline (1 ml) in a 12-well plate. SYTO 9-PI mixture (1 μl) was then added, and the plate was incubated at 37°C for 20 min. Biofilms were then washed twice with saline (1 ml), fixed with 4% PFA (200 μl), and kept at 4°C for 1 h. Biofilms were washed

again with saline (1 ml), and cover glasses were kept inverted on clean slides for imaging by CLSM (Leica TCS SP8; Leica, Germany).

Transmission electron microscopy. The effects of the amphiphiles on the membrane structures of *S. aureus* and *C. albicans* were investigated using transmission electron microscopy (35, 37). Planktonic samples (log-phase cultures) of *C. albicans* (10^6 CFU) as well as *S. aureus* (10^5 CFU) were treated with CAP 3 at 8 μ M (for *S. aureus*) and 4 μ M (for *C. albicans*) for 2 h, 6 h, and 12 h. After treatment, both untreated and treated cells of *C. albicans* and *S. aureus* were fixed with a mixture of 2.5% glutaraldehyde and 4% paraformaldehyde (100 μ l) for 30 min each followed by a gradient dehydration with ethanol. Next, the cells were embedded in Epon 812 resin post, and cells in ultrathin sections were stained by a mixture of uranyl acetate and lead citrate. Imaging was carried out on a Tecnai G2 20 twin (FEI) transmission electron microscope. For microscopic image analysis, images from different fields of view were quantified by manually counting the numbers of normal and affected cells (cells with evident shrinkage of cytoplasm). This was a blinded study carried out by different authors, and the data are presented after performing statistical analysis for both *S. aureus* and *C. albicans*.

Scanning electron microscopy. We prepared the samples for scanning electron microscopy (SEM) using a modified version of the previously published protocol (15). Biofilms (*C. albicans*, *S. aureus*, and polymicrobial) were formed on cover glasses as described above and treated with CAP 3 for 24 h at 16 μ M for *C. albicans*, 32 μ M for *S. aureus*, and 32 μ M for polymicrobial biofilms. Biofilms were washed with PBS (1 ml) two times to remove unbound biofilm components and debris and fixed with 4% PFA (100 μ l) for 1 h. Biofilms were again washed with PBS (1 ml) followed by gradient dehydration comprising successive 5 min incubations in 50%, 70%, and 95% ethanol and lastly a 10 min incubation in 100% ethanol (1 ml). Following dehydration, cover glasses were air dried, mounted upright on stubs with double-sided carbon tape, and coated with gold before imaging on an Evo 18, Zeiss scanning electron microscope. The voltage used was 15 kV, and magnifications were $\times 3,500$, $\times 7,500$, and $\times 10,000$.

Animal studies. (i) Ethics statement. All animal experiments were performed after obtaining ethical approval from the Institutional Animal Ethics Committee of Regional Centre for Biotechnology (RCB/IAEC/2016/001, RCB/IAEC/2016/10, and RCB/IAEC/2017/015).

(ii) Wound infection model. For the *S. aureus* wound infection model, we used the published protocol (56). Male BALB/c mice (6 to 8 weeks old) were housed in three cages ($n = 3$ /group) and designated untreated (saline treated), neomycin treated (40 mg/kg), and CAP 3 treated (40 mg/kg). The hair of the mice was trimmed and shaved at the region of interest prior to the day of infection. Their skin was swabbed with povidone iodine solution followed by 70% ethanol, and an incision of ~ 1 -cm diameter was made by removing the upper skin on the back of the mice using sterilized dissecting scissors and forceps. Bacterial culture (30 μ l in saline) from an inoculum of overnight culture supplemented with kanamycin (200 μ g/ml) was applied over the wound to induce infection (10^6 CFU/mice), and treatment was started after 18 h of infection. Mice were treated three times a day for 4 days. On day 5, mice were euthanized, and their skin was aseptically removed, weighed, and homogenized. The tissue homogenates were serially diluted in normal saline, plated on LB-kanamycin plates, and incubated for 24 h before colonies were counted. Data are expressed as means \pm standard deviations (SDs).

For the *C. albicans* wound infection model, we used a neutropenic infection model (41, 57). Two doses of cyclophosphamide (150 mg/kg 4 days before infection and 100 mg/kg 1 day before infection) were given to mice to make them neutropenic. Mice were segregated ($n = 3$ /group) and housed as mentioned above. They were subjected to a wound infection of 30 μ l in saline from an inoculum (of overnight culture of *C. albicans* on day 0 [10^6 CFU/mice]), and treatment was started after 18 h of infection. Mice in groups 2 and 3 were treated with fluconazole (40 mg/kg, thrice a day) and CAP 3 (40 mg/kg, thrice a day), respectively, for 3 days. On day 4, tissues from infected areas were excised, homogenized in saline, serially diluted, and plated on YPD agar plates supplemented with ampicillin (100 μ g/ml). Plates were incubated at 30°C for 2 days, and the colonies were counted. Data are expressed as means \pm SDs.

The polymicrobial wound infection model was carried out in neutropenic mice ($n = 3$ /group) using an inoculum of *S. aureus* (30 μ l, 10^6 CFU/mice) and *C. albicans* (30 μ l, 10^5 CFU/mice). Group 1 mice were left untreated, and mice in group 2 were treated with combination of neomycin (40 mg/kg) and fluconazole (40 mg/kg) (NeoF) thrice a day for 3 days. Group 3 mice were treated with CAP 3 (40 mg/kg, thrice a day) for 3 days. For the CFU assay, skin tissues were excised and weighed, and homogenates were plated on LB-kanamycin and YPD-ampicillin plates to enumerate the colonies of *S. aureus* and *C. albicans*. The LB agar plates were incubated at 37°C for 24 h, and YPD agar plates were incubated at 30°C for 48 h before counting the colonies and analyzing the data. Data are expressed as means \pm SDs.

(iii) Catheter infection model. For catheter infections (58), BALB/c mice (6 to 8 weeks old) were randomized into three groups of 3 mice each. Uncoated and DCM- and CAP 3-coated catheters (~ 0.5 cm in size) were inserted subcutaneously into mice in each group, followed by infection (30 μ l in saline, 10^6 CFU/mice) with an inoculum from an overnight culture of bacteria. Cuts were then resealed with Dermabond. On day 6, bioluminescence imaging was performed to quantify the formation of biofilms using and *in vivo* imaging system (IVIS) (IVIS Spectrum; Perkin-Elmer, USA). After imaging, mice were euthanized and their skin was aseptically removed. Catheters were taken out and dipped in saline (1 ml) to remove planktonic bacteria followed by vortexing (30 to 40 min) with intermittent sonication. The suspensions were serially diluted in saline and plated on LB-kanamycin plates. Plates were incubated for 24 h at 37°C and colonies were counted. Similarly, *C. albicans* catheter infection ($n = 4$ /group) using 30 μ l in saline (10^6 CFU/mice) and polymicrobial infection studies ($n \geq 3$ /group) using 30 μ l in saline (10^5 CFU of *C. albicans* and 10^6 CFU of *S. aureus*/mice) were performed using neutropenic mice, and imaging and CFU analyses were performed. For bioluminescence imaging of *C. albicans*, luciferin substrate (30 μ l of 5 mg/ml) was injected via a needle over the catheter.

Spectral unmixing and data analysis. Spectral unmixing and data analysis were as described (59). Before starting the unmixing from polymicrobial infected mice, we generated a library of bacterial *S. aureus* Xen 36 and pACT1:*luc*_{OPT} (3B10) bioluminescence by manual unmixing using the software. To generate the library, different sets of mice were infected with Xen 36 and pACT1:*luc*_{OPT} (3B10) separately and imaged under spectral unmixing mode in IVIS Spectrum (42, 43). Xen 36 has an emission maximum at 489 nm and pACT1:*luc*_{OPT} (3B10) has its emission maximum at 612 nm. For experimental imaging, we selected two different spectra for Xen 36 and pACT1:*luc*_{OPT} (3B10), took images, and manually assigned the spectra. We acquired images of experimental mice after injecting D-luciferin substrate in spectral unmixing mode in IVIS Spectrum. We used the constructed spectral data library and reloaded the same for unmixing the Xen 36 and pACT1:*luc*_{OPT} (3B10) bioluminescence from the polymicrobial infected mice to acquire and quantify unmixed images. After unmixing, the intensity of bioluminescence of bacteria and fungi was quantified and plotted. Data are reported as means \pm SDs.

ACKNOWLEDGMENTS

This work was supported by intramural funding from the Regional Centre for Biotechnology, Amity University, Haryana, and the Department of Biotechnology, Government of India. Research in the lab of A.B. is supported by BT/PR12297/MED/29/895/2014 (DBT), BT/PR17525/MED/29/1021/2016 (DBT), and BT/PR27264/Med/29/1277/2018 (DBT). A. Saini is supported by BT/PR17525/MED/29/1021/2016 (DBT). S.G. is supported by the RCB-Young investigator program. P.S.Y. and S.P. were supported by research fellowships from UGC, and K.Y. and S.K. were supported by research fellowships from RCB. The small animal facility at the Regional Centre for Biotechnology is supported by BT/PR5480/INF/22/158/2012 (DBT).

We thank Alistair J. P. Brown, University of Aberdeen, UK, and Sudha Komath, School of Life Sciences, Jawaharlal Nehru University, New Delhi, India, for the EGFP-expressing *Candida albicans* BWP17 strain. We also thank Matthias Brock, University of Nottingham (UK), and the Hans-Knöll-Institute Jena (Germany) for providing the bioluminescent *Candida albicans* strain pACT1:*luc*_{OPT} (3B10). We thank Addgene for mCitrine-pBAD (plasmid 54723) and pCypet-His (plasmid 14030) plasmids. We also thank the DBT e-Library Consortium (DeLCON) for providing access to e-resources.

We declare no conflicts of interests.

S.G. performed all biofilm experiments. J.T. and S.P. performed animal studies. R.G., A. Saini, and K.Y. performed *in vitro* bacterial and fungal studies. S.K. and D.M. synthesized the compounds. P.S.Y. and M.V. standardized the initial biofilm and animal experiments. R.P. supervised the initial screening of amphiphiles for antifungal activities. A. Singh supervised the TEM studies. A. Srivastava supervised the SEM studies. S.G. and A.B. conceived and supervised the project.

REFERENCES

- Peters BM, Jabra-Rizk MA, O'May GA, Costerton JW, Shirtliff ME. 2012. Polymicrobial interactions: impact on pathogenesis and human disease. *Clin Microbiol Rev* 25:193–213. <https://doi.org/10.1128/CMR.00013-11>.
- Tay WH, Chong KKL, Kline KA. 2016. Polymicrobial–host interactions during infection. *J Mol Biol* 428:3355–3371. <https://doi.org/10.1016/j.jmb.2016.05.006>.
- Peleg AY, Hogan DA, Mylonakis E. 2010. Medically important bacterial–fungal interactions. *Nat Rev Microbiol* 8:340–349. <https://doi.org/10.1038/nrmicro2313>.
- Bertesteanu S, Triaridis S, Stankovic M, Lazar V, Chifiriuc MC, Vlad M, Grigore R. 2014. Polymicrobial wound infections: pathophysiology and current therapeutic approaches. *Int J Pharm* 463:119–126. <https://doi.org/10.1016/j.ijpharm.2013.12.012>.
- Le KY, Dastgheyb S, Ho TV, Otto M. 2014. Molecular determinants of staphylococcal biofilm dispersal and structuring. *Front Cell Infect Microbiol* 4:167. <https://doi.org/10.3389/fcimb.2014.00167>.
- Iliev ID, Leonardi I. 2017. Fungal dysbiosis: immunity and interactions at mucosal barriers. *Nat Rev Immunol* 17:635–646. <https://doi.org/10.1038/nri.2017.55>.
- Lohse MB, Gulati M, Johnson AD, Nobile CJ. 2018. Development and regulation of single- and multi-species *Candida albicans* biofilms. *Nat Rev Microbiol* 16:19–31. <https://doi.org/10.1038/nrmicro.2017.107>.
- Lynch AS, Robertson GT. 2008. Bacterial and fungal biofilm infections. *Annu Rev Med* 59:415–428. <https://doi.org/10.1146/annurev.med.59.110106.132000>.
- Harriott MM, Noverr MC. 2011. Importance of candida-bacterial polymicrobial biofilms in disease. *Trends Microbiol* 19:557–563. <https://doi.org/10.1016/j.tim.2011.07.004>.
- Kong EF, Tsui C, Kuchariková S, Andes D, Van Dijk P, Jabra-Rizk MA. 2016. Commensal protection of *Staphylococcus aureus* against antimicrobials by *Candida albicans* biofilm matrix. *mBio* 7:e01365-16. <https://doi.org/10.1128/mBio.01365-16>.
- Peters BM, Noverr MC. 2013. *Candida albicans-Staphylococcus aureus* polymicrobial peritonitis modulates host innate immunity. *Infect Immun* 81:2178–2189. <https://doi.org/10.1128/IAI.00265-13>.
- Francolini I, Donelli G. 2010. Prevention and control of biofilm-based medical-device-related infections. *FEMS Immunol Med Microbiol* 59:227–238. <https://doi.org/10.1111/j.1574-695X.2010.00665.x>.
- Kean R, Rajendran R, Haggarty J, Townsend EM, Short B, Burgess KE, Lang S, Millington O, Mackay WG, Williams C, Ramage G. 2017. *Candida albicans* mycofilms support *Staphylococcus aureus* colonization and enhances miconazole resistance in dual-species interactions. *Front Microbiol* 8:258. <https://doi.org/10.3389/fmicb.2017.00258>.
- Koo H, Allan RN, Howlin RP, Stoodley P, Hall-Stoodley L. 2017. Targeting microbial biofilms: current and prospective therapeutic strategies. *Nat Rev Microbiol* 15:740–755. <https://doi.org/10.1038/nrmicro.2017.99>.
- Harriott MM, Noverr MC. 2009. *Candida albicans* and *Staphylococcus*

- aureus* form polymicrobial biofilms: effects on antimicrobial resistance. *Antimicrob Agents Chemother* 53:3914–3922. <https://doi.org/10.1128/AAC.00657-09>.
16. Hancock RE, Diamond G. 2000. The role of cationic antimicrobial peptides in innate host defences. *Trends Microbiol* 8:402–410. [https://doi.org/10.1016/S0966-842X\(00\)01823-0](https://doi.org/10.1016/S0966-842X(00)01823-0).
 17. De Lucca AJ, Walsh TJ. 1999. Antifungal peptides: novel therapeutic compounds against emerging pathogens. *Antimicrob Agents Chemother* 43:1–11. <https://doi.org/10.1128/AAC.43.1.1>.
 18. Rautenbach M, Troskie AM, Vosloo JA. 2016. Antifungal peptides: to be or not to be membrane active. *Biochimie* 130:132–145. <https://doi.org/10.1016/j.biochi.2016.05.013>.
 19. Matejuk A, Leng Q, Begum MD, Woodle MC, Scaria P, Chou S-T, Mixson AJ. 2010. Peptide-based antifungal therapies against emerging infections. *Drugs Future* 35:197. <https://doi.org/10.1358/dof.2010.035.03.1452077>.
 20. Nicolas P, Mor A. 1995. Peptides as weapons against microorganisms in the chemical defense system of vertebrates. *Annu Rev Microbiol* 49:277–304. <https://doi.org/10.1146/annurev.mi.49.100195.001425>.
 21. Reen FJ, Phelan JP, Gallagher L, Woods DF, Shanahan RM, Cano R, Ó Muimhneacháin E, McGlacken GP, O’Gara F. 2016. Exploiting interkingdom interactions for development of small-molecule inhibitors of *Candida albicans* biofilm formation. *Antimicrob Agents Chemother* 60:5894–5905. <https://doi.org/10.1128/AAC.00190-16>.
 22. Konai MM, Haldar J. 2017. Fatty acid comprising lysine conjugates: anti-MRSA agents that display *in vivo* efficacy by disrupting biofilms with no resistance development. *Bioconjug Chem* 28:1194–1204. <https://doi.org/10.1021/acs.bioconjchem.7b00055>.
 23. Singla P, Dalal P, Kaur M, Arya G, Nimesh S, Singh R, Salunke DB. 2018. Bile acid oligomers and their combination with antibiotics to combat bacterial infections. *J Med Chem* 61:10265–10275. <https://doi.org/10.1021/acs.jmedchem.8b01433>.
 24. Ghosh C, Yadav V, Younis W, Mohammad H, Hegazy YA, Seleem MN, Sanyal K, Haldar J. 2017. Aryl-alkyl-lysines: membrane-active fungicides that act against biofilms of *Candida albicans*. *ACS Infect Dis* 3:293–301. <https://doi.org/10.1021/acs.infectdis.6b00192>.
 25. Bera S, Zhanel GG, Schweizer F. 2008. Design, synthesis, and antibacterial activities of neomycin-lipid conjugates: polycationic lipids with potent gram-positive activity. *J Med Chem* 51:6160–6164. <https://doi.org/10.1021/jm800345u>.
 26. Nonappa MU. 2008. Unlocking the potential of bile acids in synthesis, supramolecular/materials chemistry and nanoscience. *Org Biomol Chem* 6:657–669. <https://doi.org/10.1039/b714475j>.
 27. Lai X-Z, Feng Y, Pollard J, Chin JN, Rybak MJ, Bucki R, Epand RF, Epand RM, Savage PB. 2008. Ceragenins: cholic acid-based mimics of antimicrobial peptides. *Acc Chem Res* 41:1233–1240. <https://doi.org/10.1021/ar700270t>.
 28. Bansal S, Singh M, Kidwai S, Bhargava P, Singh A, Sreekanth V, Singh R, Bajaj A. 2014. Bile acid amphiphiles with tunable head groups as highly selective antitubercular agents. *Medchemcomm* 5:1761–1768. <https://doi.org/10.1039/C4MD00303A>.
 29. Yadav K, Yavvari PS, Pal S, Kumar S, Mishra D, Gupta S, Mitra M, Soni V, Khare N, Sharma P, Srikanth CV, Kapil A, Singh A, Nandicoori VK, Bajaj A. 2019. Oral delivery of cholic acid-derived amphiphile helps in combating *Salmonella*-mediated gut infection and inflammation. *Bioconjug Chem* 30:721–732. <https://doi.org/10.1021/acs.bioconjchem.8b00880>.
 30. Yadav K, Kumar S, Mishra D, Asad M, Mitra M, Yavvari PS, Gupta S, Vedantham M, Ranga P, Komalla V, Pal S, Sharma P, Kapil A, Singh A, Singh N, Srivastava A, Thukral L, Bajaj A. 2019. Deciphering the role of intramolecular networking in cholic acid-peptide conjugates (CAPs) at lipopolysaccharide surface in combating gram-negative bacterial infections. *J Med Chem* 62:1875–1886. <https://doi.org/10.1021/acs.jmedchem.8b01357>.
 31. Clinical and Laboratory Standards Institute. 2012. Methods for dilution antimicrobial susceptibility tests for bacteria that grow aerobically: approved standard M7-A6. Clinical and Laboratory Standards Institute, Wayne, PA.
 32. Clinical and Laboratory Standards Institute. 2012. Reference method for broth dilution antifungal susceptibility testing of yeasts: 4th informational supplement. M27-S4. Clinical and Laboratory Standards Institute, Wayne, PA.
 33. Sims PJ, Waggoner AS, Wang C-H, Hoffman JF. 1974. Mechanism by which cyanine dyes measure membrane potential in red blood cells and phosphatidylcholine vesicles. *Biochemistry* 13:3315–3330. <https://doi.org/10.1021/bi00713a022>.
 34. Stiefel P, Schmidt-Emrich S, Maniura-Weber K, Ren Q. 2015. Critical aspects of using bacterial cell viability assays with the fluorophores SYTO9 and propidium iodide. *BMC Microbiol* 15:36. <https://doi.org/10.1186/s12866-015-0376-x>.
 35. Hartmann M, Berditsch M, Hawecker J, Ardakani MF, Gerthsen D, Ulrich AS. 2010. Damage of the bacterial cell envelope by antimicrobial peptides gramicidin S and PGLa as revealed by transmission and scanning electron microscopy. *Antimicrob Agents Chemother* 54:3132–3242. <https://doi.org/10.1128/AAC.00124-10>.
 36. Niemirowicz K, Durnaś B, Tokajuk G, Piktel E, Michalak G, Gu X, Kulakowska A, Savage PB, Bucki R. 2017. Formulation and candidacidal activity of magnetic nanoparticles coated with cathelicidin LL-37 and ceragenin CSA-13. *Sci Rep* 7:4610. <https://doi.org/10.1038/s41598-017-04653-1>.
 37. Menzel LP, Chowdhury HM, Masso-Silva JA, Ruddick W, Falkovsky K, Vorona R, Malsbary A, Cherabuddi K, Ryan LK, DiFranco KM, Brice DC, Costanzo MJ, Weaver D, Freeman KB, Scott RW, Diamond G. 2017. Potent *in vitro* and *in vivo* antifungal activity of a small molecule host defense peptide mimic through a membrane-active mechanism. *Sci Rep* 7:4353. <https://doi.org/10.1038/s41598-017-04462-6>.
 38. Konai MM, Adhikary U, Samaddar S, Ghosh C, Haldar J. 2015. Structure-activity relationship of amino acid tunable lipidated norspermidine conjugates: disrupting biofilms with potent activity against bacterial persisters. *Bioconjug Chem* 26:2442–2453. <https://doi.org/10.1021/acs.bioconjchem.5b00494>.
 39. Blondeau JM. 2009. New concepts in antimicrobial susceptibility testing: the mutant prevention concentration and mutant selection window approach. *Vet Dermatol* 20:383–396. <https://doi.org/10.1111/j.1365-3164.2009.00856.x>.
 40. Hoque J, Konai MM, Sequeira SS, Samaddar S, Haldar J. 2016. Antibacterial and antibiofilm activity of cationic small molecules with spatial positioning of hydrophobicity: an *in vitro* and *in vivo* evaluation. *J Med Chem* 59:10750–10762. <https://doi.org/10.1021/acs.jmedchem.6b01435>.
 41. Hope WW, Drusano GL, Moore CB, Sharp A, Louie A, Walsh TJ, Denning DW, Warn PA. 2007. Effect of neutropenia and treatment delay on the response to antifungal agents in experimental disseminated candidiasis. *Antimicrob Agents Chemother* 51:285–295. <https://doi.org/10.1128/AAC.00601-06>.
 42. Walton KD, Lord A, Kendall LV, Dow SW. 2014. Comparison of 3 real-time, quantitative murine models of staphylococcal biofilm infection by using *in vivo* bioluminescent imaging. *Comp Med* 64:25–33.
 43. Jacobsen ID, Lüttich A, Kurza O, Hube B, Brock M. 2014. *In vivo* imaging of disseminated murine *Candida albicans* infection reveals unexpected host sites of fungal persistence during antifungal therapy. *J Antimicrob Chemother* 69:2785–2796. <https://doi.org/10.1093/jac/dku198>.
 44. Klotz SA, Chasin BS, Powell B, Gaur NK, Lipke PN. 2007. Polymicrobial bloodstream infections involving *Candida* species: analysis of patients and review of the literature. *Diagn Microbiol Infect Dis* 59:401–406. <https://doi.org/10.1016/j.diagmicrobio.2007.07.001>.
 45. Griesbeck O, Baird GS, Campbell RE, Zacharias DA, Tsien RY. 2001. Reducing the environmental sensitivity of yellow fluorescent protein. Mechanism and applications. *J Biol Chem* 276:29188–29194. <https://doi.org/10.1074/jbc.M102815200>.
 46. Yarlagaadda V, Konai MM, Paramanandham K, Nimita VC, Shome BR, Haldar J. 2015. *In vivo* efficacy and pharmacological properties of a novel glycopeptide (YV4465) against vancomycin-intermediate *Staphylococcus aureus*. *Int J Antimicrob Agents* 46:446–450. <https://doi.org/10.1016/j.ijantimicag.2015.05.014>.
 47. Canton E, Peman J, Gobernado M, Viudes A, Espinel-Ingroff A. 2004. Patterns of amphotericin B killing kinetics against seven *Candida* species. *Antimicrob Agents Chemother* 48:2477–2482. <https://doi.org/10.1128/AAC.48.7.2477-2482.2004>.
 48. Yarlagaadda V, Akkapeddi P, Manjunath GB, Haldar J. 2014. Membrane active vancomycin analogues: a strategy to combat bacterial resistance. *J Med Chem* 57:4558–4568. <https://doi.org/10.1021/jm500270w>.
 49. Alvarez-Barrientos A, Arroyo J, Canton R, Nombela C, Sánchez-Pérez M. 2000. Applications of flow cytometry to clinical microbiology. *Clin Microbiol Rev* 13:167–195. <https://doi.org/10.1128/cmr.13.2.167-195.2000>.
 50. Christensen GD, Simpson WA, Younger JJ, Baddour LM, Barrett FF, Melton DM, Beachey EH. 1985. Adherence of coagulase-negative staphylococci to plastic tissue culture plates: a quantitative model for the

- adherence of staphylococci to medical devices. *J Clin Microbiol* 22: 996–1006.
51. Chandra J, Kuhn DM, Mukherjee PK, Hoyer LL, McCormick T, Ghannoum MA. 2001. Biofilm formation by the pathogen *C. albicans*: development, architecture, and drug resistance. *J Bacteriol* 183:5385–5394. <https://doi.org/10.1128/JB.183.18.5385-5394.2001>.
 52. Budzyńska A, Różalska S, Sadowska B, Różalska B. 2017. *Candida albicans/Staphylococcus aureus* dual-species biofilm as a target for the combination of essential oils and fluconazole or mupirocin. *Mycopathologia* 182:989–995. <https://doi.org/10.1007/s11046-017-0192-y>.
 53. Weiss EC, Zielinska A, Beenken KE, Spencer HJ, Daily SJ, Smeltzer MS. 2009. Impact of *sarA* on daptomycin susceptibility of *Staphylococcus aureus* biofilms *in vivo*. *Antimicrob Agents Chemother* 53:4096–4102. <https://doi.org/10.1128/AAC.00484-09>.
 54. Hawser SP, Douglas LJ. 1994. Biofilm formation by *Candida* species on the surface of catheter materials *in vitro*. *Infect Immun* 62:915–921.
 55. Berney M, Hammes F, Bosshard F, Weilenmann H, Egli T. 2007. Assessment and interpretation of bacterial viability by using the LIVE/DEAD BacLight kit in combination with flow cytometry. *Appl Environ Microbiol* 73:3283–3290. <https://doi.org/10.1128/AEM.02750-06>.
 56. Gisby J, Bryant J. 2000. Efficacy of a new cream formulation of mupirocin: comparison with oral and topical agents in experimental skin infections. *Antimicrob Agents Chemother* 44:255–260. <https://doi.org/10.1128/aac.44.2.255-260.2000>.
 57. Conti HR, Huppler AR, Whibley N, Gaffen SL. 2014. Animal models for candidiasis. *Curr Protoc Immunol* 105:19.6.1–6.17. <https://doi.org/10.1002/0471142735.im1906s105>.
 58. Rupp ME, Ulphani JS, Fey PD, Bartscht K, Mack D. 1999. Characterization of the importance of polysaccharide intercellular adhesin/hemagglutinin of *Staphylococcus epidermidis* in the pathogenesis of biomaterial-based infection in a mouse foreign body infection model. *Infect Immun* 67: 2627–2632.
 59. Cool SK, Breyne K, Meyer E, De Smedt SC, Sanders NN. 2013. Comparison of *in vivo* optical systems for bioluminescence and fluorescence imaging. *J Fluoresc* 23:909–920. <https://doi.org/10.1007/s10895-013-1215-9>.